

MICROCOPY RESOLUTION TEST CHART  
NATIONAL BUREAU OF STANDARDS 1963-A

12

AD-A163 882

# Partial-Discharge Tests of Multiwinding High-Voltage Transformers for Space TWTAs

Prepared by

F. HAI and K. W. PASCHEN  
Materials Sciences Laboratory  
Laboratory Operations  
The Aerospace Corporation  
El Segundo, CA 90245

DTIC  
SELECTE  
FEB 10 1986  
D

23 September 1985

APPROVED FOR PUBLIC RELEASE;  
DISTRIBUTION UNLIMITED

FILE COPY

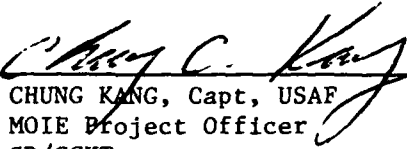
Prepared for  
SPACE DIVISION  
AIR FORCE SYSTEMS COMMAND  
Los Angeles Air Force Station  
P.O. Box 92960, Worldway Postal Center  
Los Angeles, CA 90009-2960

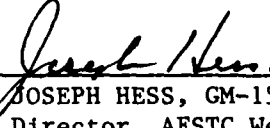
This report was submitted by The Aerospace Corporation, El Segundo, CA 90245, under Contract No. F04701-83-C-0084 with the Space Division, P.O. Box 92960, Worldway Postal Center, Los Angeles, CA 90009-2960. It was reviewed and approved for The Aerospace Corporation by R. W. Fillers, Director, Materials Sciences Laboratory.

Capt Chung Kang, SD/CGXT, was the project officer for the Mission-Oriented Investigation and Experimentation (MOIE) Program.

This report has been reviewed by the Public Affairs Office (PAS) and is releasable to the National Technical Information Service (NTIS). At NTIS, it will be available to the general public, including foreign nationals.

This technical report has been reviewed and is approved for publication. Publication of this report does not constitute Air Force approval of the report's findings or conclusions. It is published only for the exchange and stimulation of ideas.

  
CHUNG KANG, Capt, USAF  
MOIE Project Officer  
SD/CGXT

  
JOSEPH HESS, GM-15  
Director, AFSTC West Coast Office  
AFSTC/WCO OL-AB

UNCLASSIFIED

SECURITY CLASSIFICATION OF THIS PAGE (When Data Entered)

REPORT DOCUMENTATION PAGE		READ INSTRUCTIONS BEFORE COMPLETING FORM
1. REPORT NUMBER SD-TR-85-64	2. GOVT ACCESSION NO. <b>AD-A163882</b>	3. RECIPIENT'S CATALOG NUMBER
4. TITLE (and Subtitle) PARTIAL-DISCHARGE TESTS OF MULTIWINDING HIGH-VOLTAGE TRANSFORMERS FOR SPACE TWTAs	5. TYPE OF REPORT & PERIOD COVERED	
	6. PERFORMING ORG. REPORT NUMBER TR-0084A(5935-03)-1	
7. AUTHOR(s) Francis Hai and Kenneth W. Paschen	8. CONTRACT OR GRANT NUMBER(s) F04701-83-C-0084	
	9. PERFORMING ORGANIZATION NAME AND ADDRESS The Aerospace Corporation El Segundo, Calif. 90245	
11. CONTROLLING OFFICE NAME AND ADDRESS Space Division Los Angeles Air Force Station Los Angeles, Calif. 90009-2960	10. PROGRAM ELEMENT, PROJECT, TASK AREA & WORK UNIT NUMBERS	
	12. REPORT DATE 23 September 1985	
14. MONITORING AGENCY NAME & ADDRESS (if different from Controlling Office)	13. NUMBER OF PAGES 65	
	15. SECURITY CLASS. (of this report) Unclassified	
16. DISTRIBUTION STATEMENT (of this Report) Approved for public release; distribution unlimited.		
17. DISTRIBUTION STATEMENT (of the abstract entered in Block 20, if different from Report)		
18. SUPPLEMENTARY NOTES		
19. KEY WORDS (Continue on reverse side if necessary and identify by block number) Cavity defects High-voltage transformer testing Partial-discharge tests Paschen breakdown Polymer insulation		
20. ABSTRACT (Continue on reverse side if necessary and identify by block number) The high-voltage transformer is a key component in the power supply, converting a single low voltage from the power bus of a communication satellite to multiple high voltages required by a traveling-wave tube amplifier (TWTA). Partial-discharge (corona) tests are performed on this component to establish high-voltage integrity and to screen out units with high-voltage defects. These defects are usually voids and cracks occurring in the insulation of the transformer.		

UNCLASSIFIED

SECURITY CLASSIFICATION OF THIS PAGE(When Data Entered)

19. KEY WORDS (Continued)

20. ABSTRACT (Continued)

This report describes investigations conducted to determine how to perform effective partial-discharge tests (PDTs) on transformers to screen out defective units. The aspects of partial-discharge testing that were examined include (1) the test medium (air, vacuum, or dielectric fluid); (2) the test mode (60 Hz ac, ac on dc, or dc); (3) the test configuration (i.e., the testing of each insulation barrier in sequence or the simultaneous testing of all barriers); (4) test voltage magnitude (to four times the operating voltage); (5) test data; and (6) pass/fail criteria.

Destructive physical analysis (DPA) was performed on both defective and defect-free transformers to confirm the effectiveness of the recommended PDT procedures. ←

To correlate the results of PDTs with those of DPA, a simple model of discharges occurring across a planar gap was constructed, taking into consideration the gas breakdown curve (the Paschen curve), crack width, barrier width, the dielectric constant of the insulation, and the barrier voltage. Analyses based on this model related corona inception voltage monitored during PDT to crack size and location, as revealed by DPA. Similar analysis confirmed the need to test to four times the operating voltage to detect mil-size defects in certain transformer locations.

UNCLASSIFIED

SECURITY CLASSIFICATION OF THIS PAGE(When Data Entered)

PREFACE

The authors wish to thank F. M. Wachi and C. N. Su for performing the DPAs and providing the cross-section photographs used in this report.



Accession For	
NTIS CRA&I	<input checked="" type="checkbox"/>
DTIC TAB	<input type="checkbox"/>
Unannounced	<input type="checkbox"/>
Justification	
By	
Distribution /	
Availability Codes	
Dist	Avail and/or Special
A-1	

## CONTENTS

PREFACE.....	1
I. INTRODUCTION.....	7
II. THE HIGH-VOLTAGE TRANSFORMER.....	9
A. Description.....	9
B. Electrical-Stress Distribution and Level.....	9
C. Void and Crack Defects.....	9
III. PARTIAL-DISCHARGE (CORONA) TESTS OF HIGH-VOLTAGE TRANSFORMERS.....	13
A. Test Configuration.....	15
B. Partial-Discharge (Corona) Detection System.....	15
C. Test Medium.....	18
D. Test Mode, Test Magnitude, and Test Duration.....	20
IV. PARTIAL-DISCHARGE TESTS AND DESTRUCTIVE PHYSICAL ANALYSIS OF HIGH-VOLTAGE TRANSFORMERS.....	33
A. Partial-Discharge Tests of High-Voltage Transformers SN 008 and SN 016.....	33
B. Destructive Physical Analysis of High-Voltage Transformers SN 008 and SN 016.....	36
V. MODEL OF DISCHARGES OCCURRING IN A PLANAR GAP.....	43
VI. CORRELATION OF RESULTS OF PARTIAL-DISCHARGE TESTS AND DESTRUCTIVE PHYSICAL ANALYSIS.....	47
A. Transformer SN 008.....	47
B. Transformer SN 016.....	47
C. PDT/DPA Anomalies.....	51
VII. PARTIAL-DISCHARGE TESTS OF HIGH-VOLTAGE TRANSFORMERS TO EXTRA-HIGH LEVELS.....	53
A. Reference PDT Voltage.....	53
B. PDT of SN 010 at Four Times Operating Voltage.....	53
C. PDT of Defect-Free HV Transformers.....	56
D. Concerns Regarding PDT to Four Times Operating Voltage.....	56

CONTENTS (Continued)

VIII. CONCLUSIONS.....	59
REFERENCES.....	61
APPENDIX: A MODEL FOR ESTIMATING DISCHARGE MAGNITUDES.....	63

## FIGURES

1.	Cross Section of a Multiwinding Toroidal Transformer.....	10
2.	(a) Intrawinding Test Circuit from MIL-T-27. (b) Interwinding Test Circuit from MIL-T-27.....	14
3.	(a) Test of a Single Barrier. (b) Simultaneous Test of Two Barriers.....	16
4.	Resistive Divider Test of HV Transformer.....	17
5.	Strip Chart Recording Showing Test Voltage and Discharge Activity.....	19
6.	Partial-Discharge Tests of HV Transformer in Various Media.....	21
7.	Representative HV Transformer Test Data Showing CIV, CEV, and Delay in CIV.....	30
8.	(a) General Variation of CIV with Delay Time. (b) CIV with No Delay for Same Test Sample. (c) Variation of Delay Time at Constant CIV.....	31
9.	Cross Section of HV Transformer SN 008.....	38
10.	Cross Section of HV Transformer SN 016.....	39
11.	Core Cross Section of SN 008, Showing Locations of Cracks and Voids.....	40
12.	Core Cross Section of SN 016, Showing Locations of Cracks and Voids.....	41
13.	The Paschen Curve at Atmospheric Pressure.....	44
14.	Model for Determination of Crack Voltage.....	45
15.	Conditions for CIV in HV Transformer SN 008.....	48
16.	Resistive Divider Partial-Discharge Test of HV Transformer SN 016.....	49
17.	Conditions for CIV in HV Transformer SN 016.....	50
18.	Strip Chart Recording of Partial-Discharge Test of HV Transformer SN EQM 7T.....	57

TABLES

1.	PDT Data Showing the Effect of the Test Medium.....	22
2.	PDT Data Showing Effects of AC and DC Test Voltages.....	24
3.	PDT Data Showing AC Voltage Determination of CIV and CEV.....	26
4.	PDT Data Showing the Effects of AC and DC Test Voltages.....	27
5.	PDT Data Showing the Effects of AC and DC Test Voltages on CIV and CEV.....	28
6.	Working Voltages and Test Voltages for Two HV Transformers.....	34
7.	PDT Results for HV Transformer SN 008.....	35
8.	PDT Results for HV Transformer SN 016.....	37
9.	PDT Reference Voltages.....	54
10.	PDT Voltages at Four Times the Reference Voltages.....	55

## I. INTRODUCTION

A traveling-wave tube amplifier (TWTA) is essential for high-power, high-frequency, down- and cross-link space communication. For operation of the TWTA in this system, negative-dc high voltage at several specified levels is required. These voltages are provided by the electric-power conditioner (EPC), an integral part of the TWTA which converts a single low voltage from the power bus of the communication satellite to the various high voltages. The primary component performing this conversion in the EPC (or power supply) is the high-voltage transformer.

## II. THE HIGH-VOLTAGE TRANSFORMER

### A. DESCRIPTION

The high-voltage (HV) transformer consists of multiple windings of magnet wire that has been hand-wound onto a toroidal core. A toroidal core, rather than a "C" core, is used to minimize space and weight. The size of the magnet wires used range from AWG No. 17 (0.045-in. diam) for the primary winding to AWG No. 36 (0.005-in. diam) for the secondary windings. These windings are insulated from one another by layers of polyester tape. The wound transformer is then encapsulated with an epoxy (Epon 825 with a HV hardener) in vacuum and cured at elevated temperature under high pressure. A cross section of one of the transformers used in these investigations is shown in Fig. 1. The fabrication of high-reliability transformers such as these is described in detail in Ref. 1.

### B. ELECTRICAL-STRESS DISTRIBUTION AND LEVEL

In application, the primary winding of the transformer is driven by a 10 to 20-kHz square wave having a 20 to 40-V signal. The secondary windings of various numbers of turns are connected to the HV rectifier circuits that are appropriately stacked to provide the required TWTA operating voltages, with the maximum voltage ranging to above 5 kV. This HV stack is controlled and monitored by other circuits. Therefore, the insulation barriers in these transformers are electrically stressed by both ac and dc voltages, i.e.,  $V_{total} = V_{ac}(peak) + V_{dc}$ . Furthermore, the secondary windings and the rectifier circuits can be arranged so that the dc voltage either increases monotonically outward from the transformer core, or peaks within the secondary section and then decreases toward the exterior of the transformer. The latter dc voltage distribution places less electrical stress across the insulation barrier covering the transformer.

### C. VOID AND CRACK DEFECTS

High-voltage defects can occur in the insulation barriers of these transformers during the fabrication process. These defects, usually in the form of voids and cracks, are produced by the following processing problems:



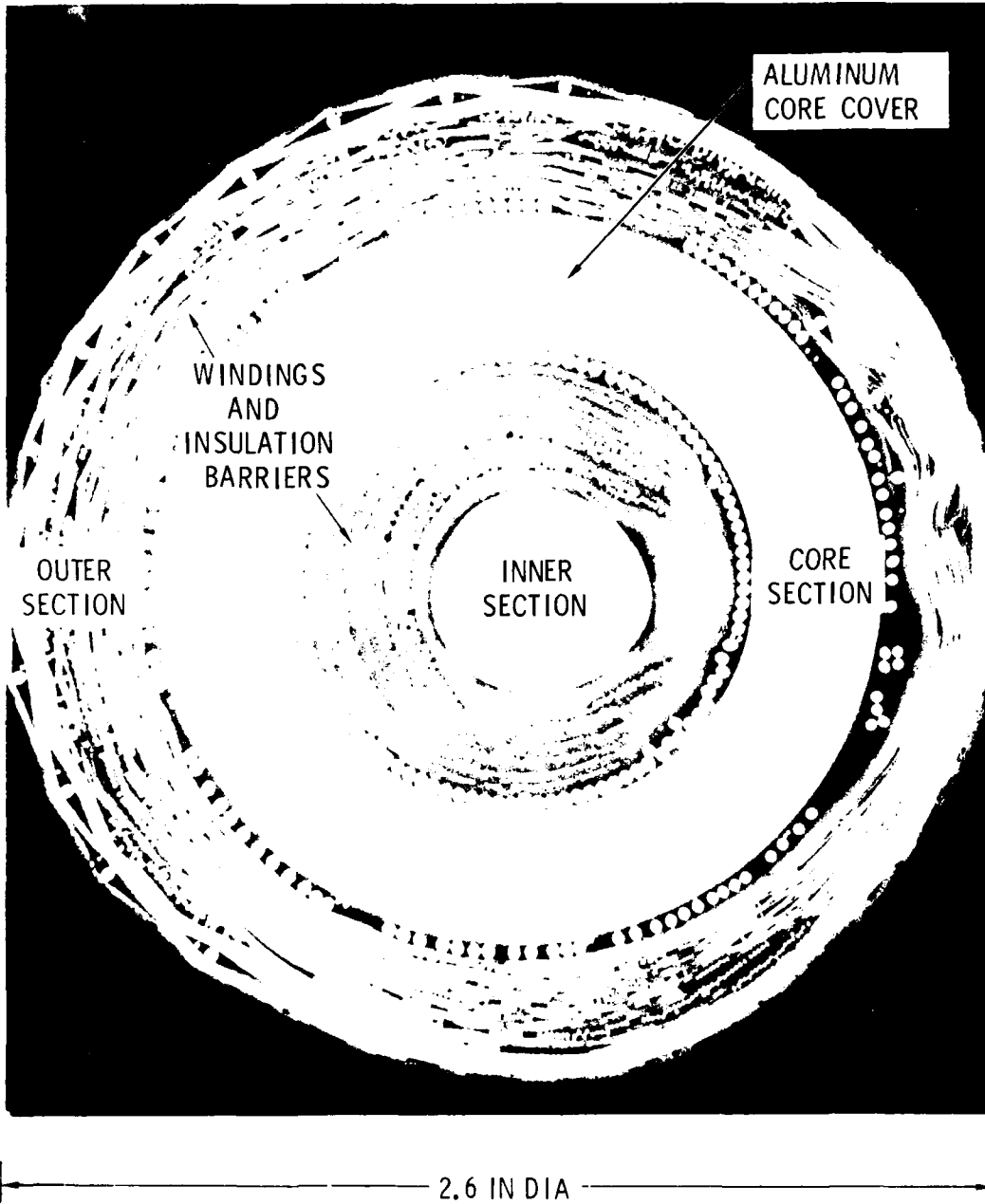


Fig. 1. Cross Section of a Multiwinding Toroidal Transformer

1. If the epoxy mixture is not sufficiently outgassed to eliminate all the low-molecular-weight volatile components, voids occur in the encapsulant.
2. If the epoxy is too viscous, it fails to penetrate the windings of the transformer, because both the epoxy and the transformer are too low in temperature. On the other hand, if the temperature is too high, the epoxy sets up too soon; this prevents the epoxy from fully penetrating the winding. Both conditions lead to voids in the encapsulant.
3. If the transformer parts are insufficiently cleaned of contamination, this contamination volatilizes during cure and produces voids in the encapsulant.
4. If the filled epoxy does not have sufficient mechanical flexibility to compensate for the difference in thermal expansion and mechanical properties between the metal and the encapsulant, cracks occur in the encapsulant.
5. If the potted transformer is allowed to gel at too high a temperature, cracks occur in the encapsulant as the transformer cools down to room temperature.
6. If the potted transformer is cured too quickly at high temperature, a very brittle unit is produced which cracks from thermal-cycle testing and operation.

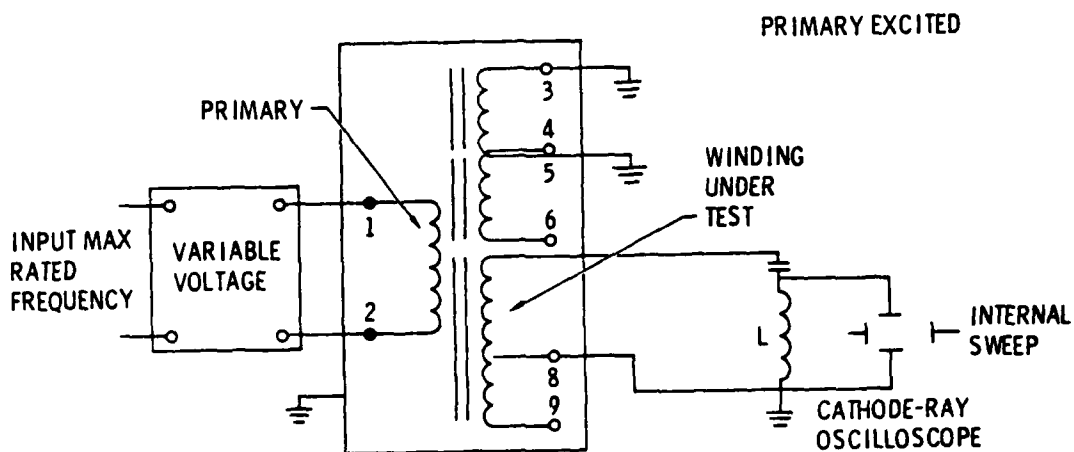
### III. PARTIAL-DISCHARGE (CORONA) TESTS OF HIGH-VOLTAGE TRANSFORMERS

High-voltage (HV) transformers with small incipient-level voids or cracks will operate in most cases satisfactorily for a short time. However, these HV transformers should not be used in space TWTAs that are expected to operate continuously and reliably for ten years in a vacuum. Moreover, these TWTAs must withstand moderately high temperatures during operation and low temperatures during storage in space. The conventional method of screening out transformers with void or crack defects has been the corona (or partial-discharge) test. This report describes investigations conducted to determine how to apply the partial-discharge test (PDT) effectively to screen out HV defects at the incipient level.

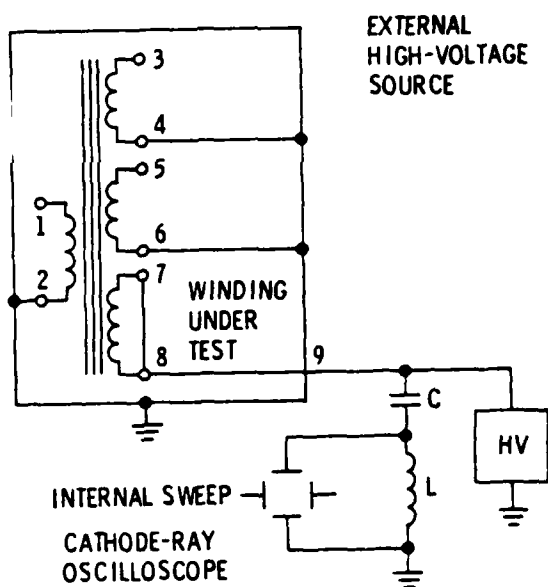
Military specification MIL-T-27 (Ref. 2) describes general requirements for transformers and inductors. Of specific interest are the corona tests for intrawinding insulation (i.e., the insulation between turns on the same winding) and for interwinding insulation (i.e., the insulation between windings). The circuits for the two tests are given in Fig. 2. For either test to be effective, sufficient electrical stress must be applied across the HV defect to produce detectable discharges (corona).

The intrawinding test (Fig. 2a) is the only test of the two that is effective in detecting defects along a winding; however, because the dc stress is absent, it is only minimally effective in detecting defects between windings. (The dc stress is produced by stacking the rectifier circuits, but the transformer is tested without these circuits, as indicated in Fig. 2a.) Nonetheless, for defects along the winding, the electrical stress is relatively low, i.e.,  $<1$  V/mil at operating voltage. Therefore, unless the void or crack defect is extensive in the direction of the winding, the voltage developed across the defect is insufficient to cause electrical breakdown, which indicates that the intrawinding test is ineffective for detecting void or crack-type defects. (Intrawinding defects are more likely to be detected by other transformer tests, such as the winding resistance or turns-ratio tests.) The intrawinding test was not used in the investigations described in this report.





A



B

Fig. 2. (a) Intrawinding Test Circuit from MIL-T-27. (b) Interwinding Test Circuit from MIL-T-27.

#### A. TEST CONFIGURATION

The MIL-T-27 interwinding test configuration is given in Fig. 2b. As indicated, the insulation barriers on both sides of the winding under test are examined simultaneously, and the occurrence of partial discharges (corona) is monitored on an oscilloscope. In the present investigations either one insulation barrier or all the barriers are examined at one time. In the test of one barrier at a time (barrier test), all the windings on one side of the barrier under test are tied together and are connected to ground potential, while all the windings on the other side are also tied together but are connected to high voltage. This test arrangement is shown schematically in Fig. 3a. The advantages of using this test arrangement rather than the one indicated in Fig. 2b are that (1) each barrier can be tested to the specified level without the possibility of overstressing an adjacent barrier (see Fig. 3b for an example of this case), and (2) if a corona is detected, there is no ambiguity as to the barrier in which it occurs. The disadvantage associated with this approach is that each barrier must be tested in sequence, which necessitates a relatively long test time for a multiwinding transformer.

In the simultaneous test of all windings, different test voltages are applied to the windings by means of a resistive voltage-divider network. This divider test, first proposed by a transformer manufacturer, is shown schematically in Fig. 4. The transformer is connected to the divider network as shown, and high voltage at the prescribed level is applied to the top of the network. The primary advantages to using this approach are that (1) all insulation barriers are realistically stressed, including the regions where the winding leads are brought out of the transformer, and (2) minimum time is needed to screen a defect-free transformer. However, if a corona is detected in this divider test, the transformer must be retested by means of the barrier test to find the defective barrier.

#### B. PARTIAL-DISCHARGE (CORONA) DETECTION SYSTEM

In the early interwinding tests performed at Aerospace, only the barrier test was used. High voltage at 60 Hz ac from a commercial step-up transformer driven by a variac was applied to the HV transformer under test. The

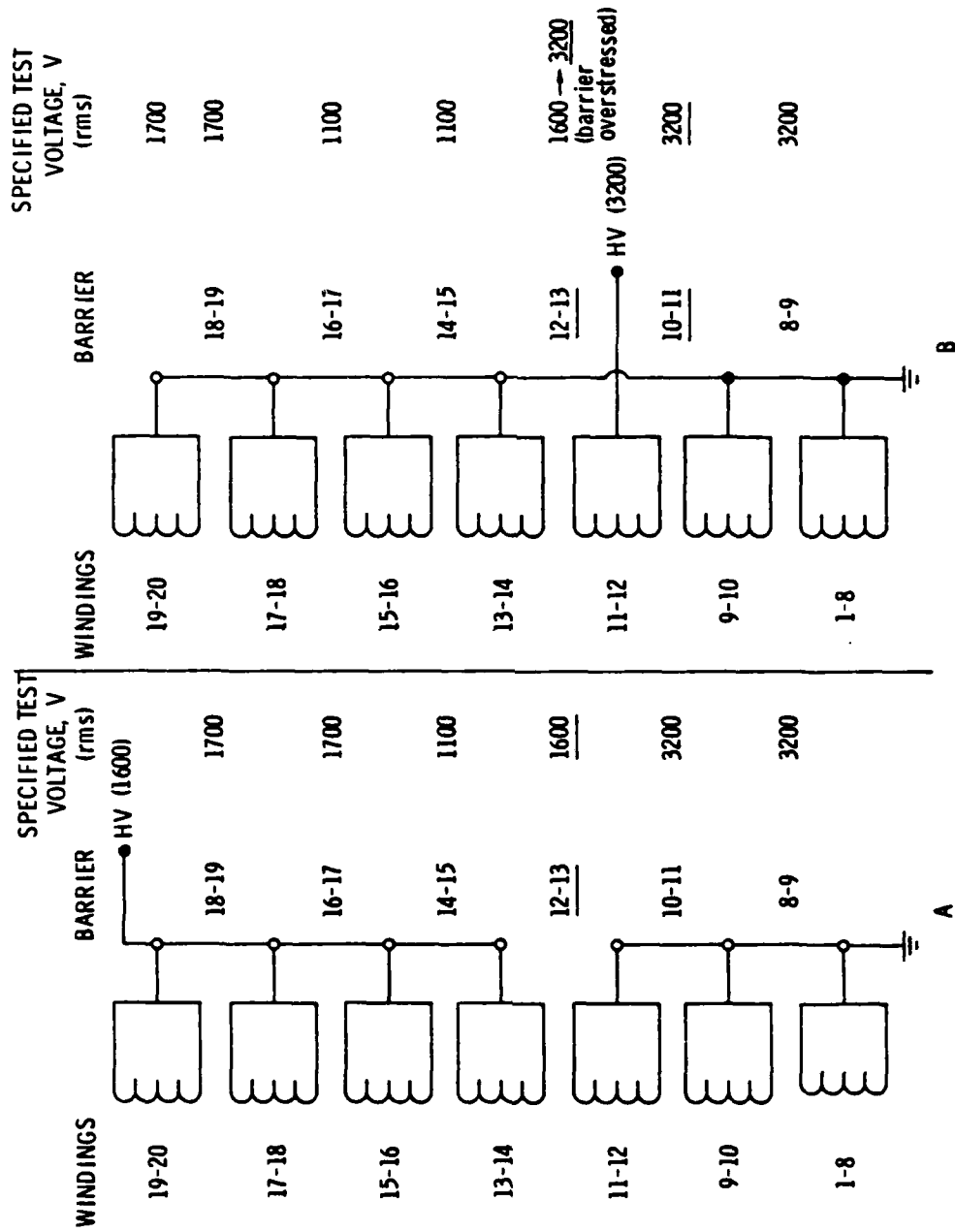


Fig. 3. (a) Test of a Single Barrier. (b) Simultaneous Test of Two Barriers.

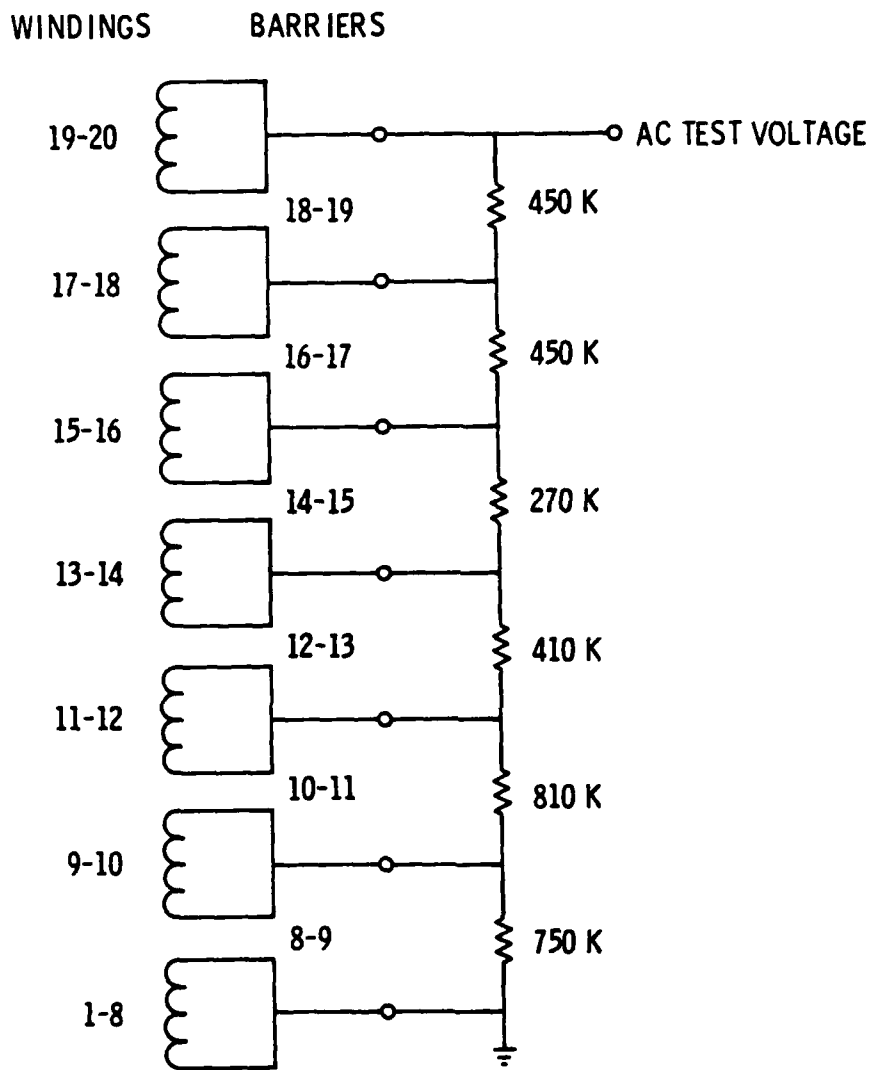


Fig. 4. Resistive Divider Test of HV Transformer

discharge activity produced was detected by the Aerospace PDT system originally designed to detect and monitor discharges occurring in the encapsulation of a traveling-wave tube (Ref. 3). This detection system was calibrated by means of the ASTM Standard D1868-73 (Ref. 4). The data, in terms of the number of discharges of specified magnitude occurring within a given time interval, are computer-processed along with indications of time, temperature, test voltage, and pressure. Samples of these output data are given below. A review of these data gives a direct indication of corona inception voltage (CIV) and corona extinction voltage (CEV).

In the later interwinding tests performed at Aerospace by means of either the barrier test or the divider test, high voltage was applied from a corona-free power supply manufactured by the Biddle Co., and discharge activity was monitored by a Biddle partial-discharge (corona) detection system. By means of the variable-speed motor-driven voltage control on the power supply, the 60-Hz ac test voltage was increased to the specified level at constant rate. This test voltage was monitored on one input of a dual-input strip-chart recorder. The other input monitored the discharge activity detected by the Biddle system. Simultaneous recording of the two inputs on the same strip chart gives an accurate indication of CIV. The CEV is determined by decreasing the test voltage at constant rate and noting the disappearance of discharge activity. A strip-chart record showing these measurements is given in Fig. 5. An attractive feature of this system is that a hard copy of the test results, giving not only an accurate indication of CIV and CEV but also an estimation of the magnitude of the discharge activity, is obtained. (The Biddle corona detection system is also equipped with an oscilloscope that can provide an elliptical trace showing the variation of discharge activity as a function of the 60-Hz sinusoidal waveform. The oscilloscope trace can also be used to monitor CIV and CEV, as indicated in Fig. 2b.)

#### C. TEST MEDIUM

The primary objective in the partial-discharge testing of an encapsulated transformer is to determine whether the unit has internal defects such as voids and cracks. At one HV transformer manufacturer, PDTs were initially

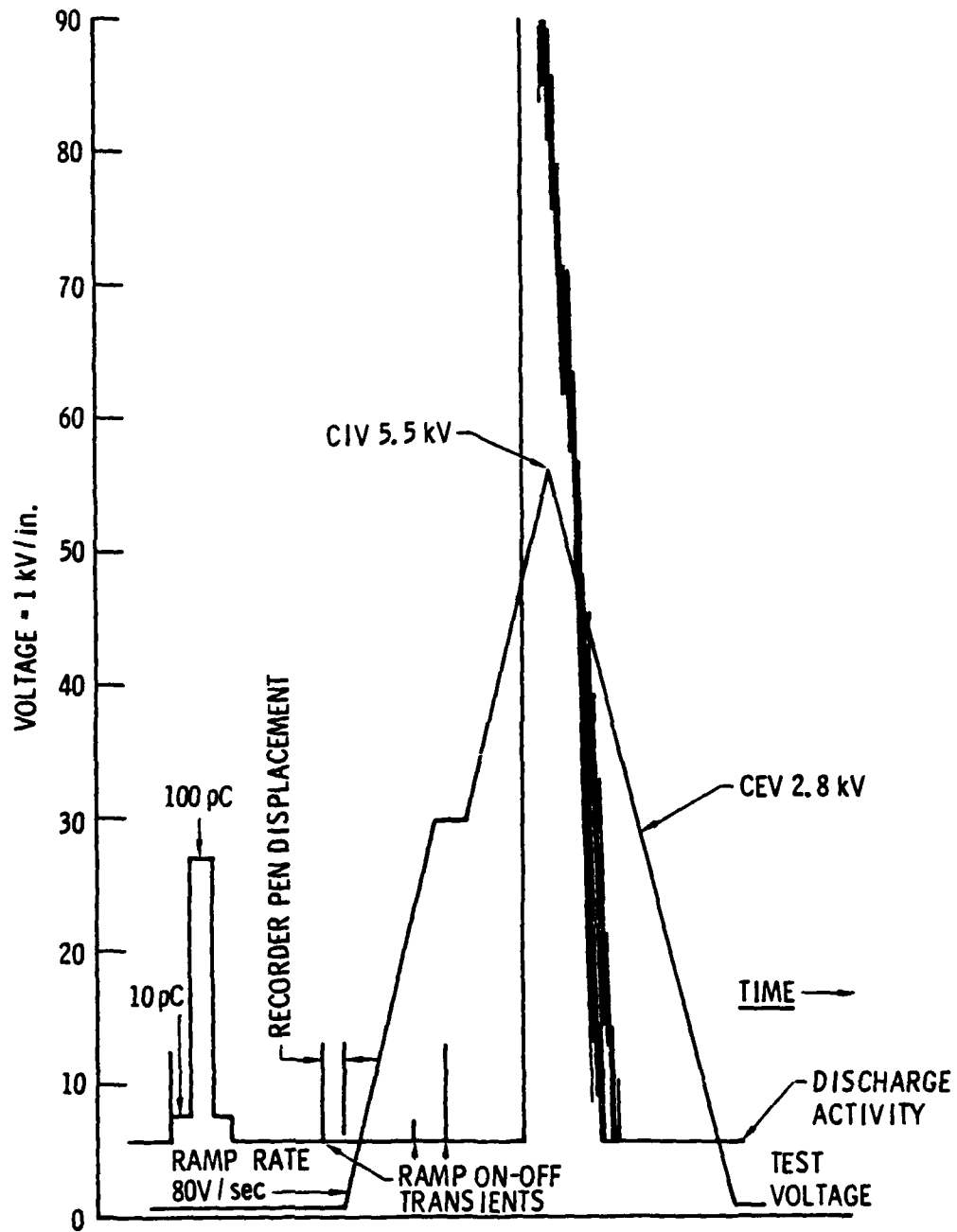


Fig. 5. Strip Chart Recording Showing Test Voltage and Discharge Activity

performed only in air. However, discharge activity monitored by PDTs in air on a transformer can come from several sources: (1) HV defects within the transformer, (2) breakdown across external surfaces, and (3) charge transfer between the surfaces of insulated wires. (Some of the HV transformers tested in these investigations have Tefzel-insulated breakout wiring, and the others have bare nickel breakout wiring.) The first source is the only one of concern because the second and third will be changed or eliminated, either by potting or conformal coating of the unit when the HV transformer is integrated into the electric-power conditioner (EPC).

To determine the effects of the test medium on the discharge signature, PDTs of a HV transformer were conducted in air, in vacuum, and in the dielectric fluid Fluorinert (FC 77). The test measurements of interest were CIV and maximum-discharge magnitude. The results are given in Fig. 6. Variation in discharge activity, usually at maximum test voltage, during the transition from air to vacuum or from air to FC 77, was also monitored. These test results are given in Table 1.

The test results indicate that PDTs of the HV transformer in air produced CIVs and discharge magnitudes higher than those produced by PDTs in vacuum or in FC 77, suggesting that some of the discharge sources were quenched by immersion of the transformer in vacuum or FC 77. These changes were confirmed by monitoring the transitions from air to vacuum and from air to FC 77, as indicated in Table 1. The results also showed in several instances that a given test voltage had to be applied for several minutes before discharge activity indicating CIV was monitored. This observation will be further noted in the following section on test magnitude and test duration.

It is recommended that PDTs of the HV transformer be conducted in the dielectric fluid FC 77 to eliminate extraneous discharge effects that can occur with tests in air. To minimize test time and equipment, tests in FC 77 are preferred to tests in vacuum.

#### D. TEST MODE, TEST MAGNITUDE, AND TEST DURATION

Insulation in the HV transformer is stressed by both ac and dc voltages. MIL-T-27 covers this case by specifying that the test voltage be

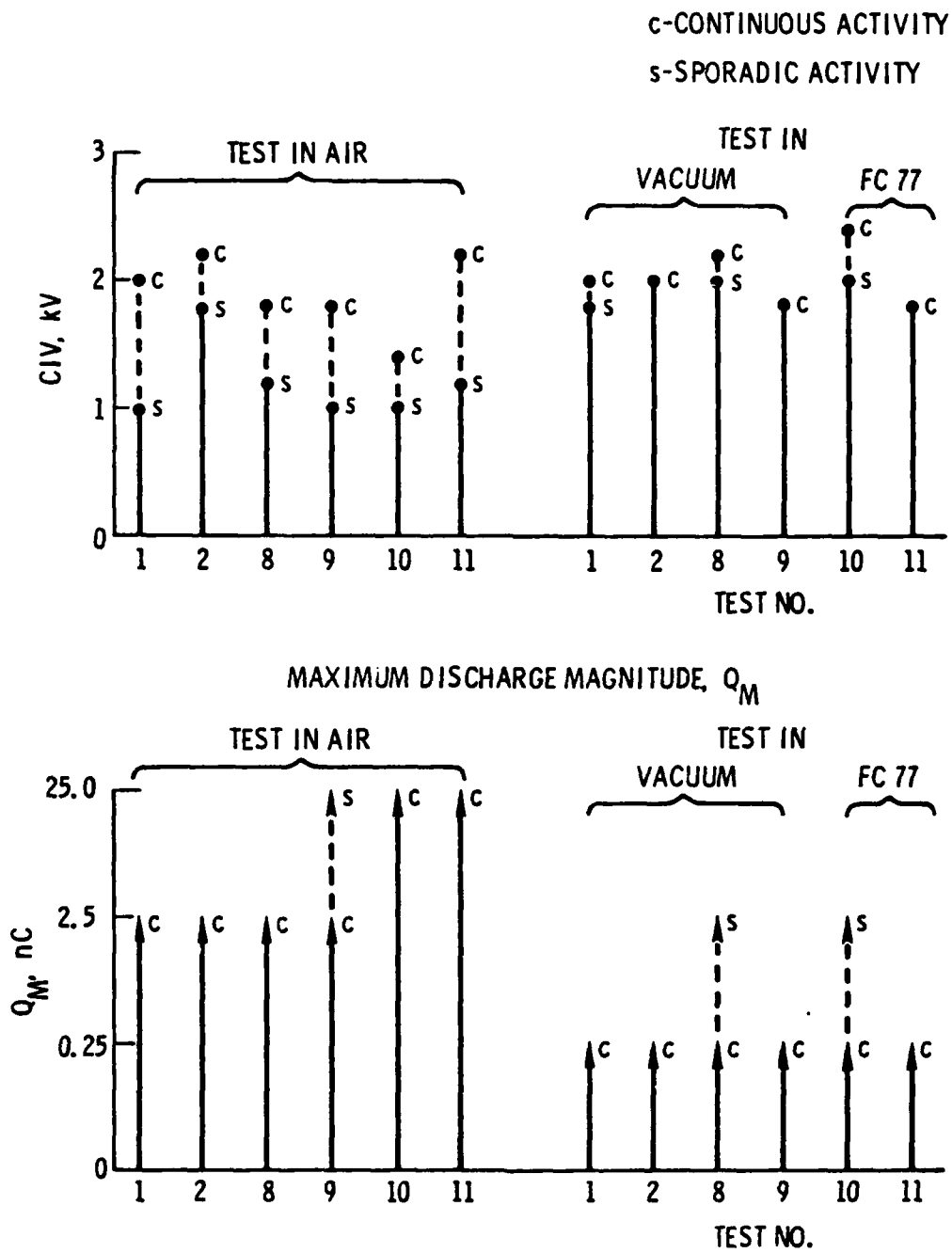


Fig. 6. Partial-Discharge Tests of HV Transformer in Various Media

Table 1. PDT Data Showing the Effects of the Test Medium. AC PDT of T-2 (11-12 to 7-8). Time period is 100 sec. Note disappearance of Ch. 4 and Ch. 5 discharge activity.

(a) Transition from Atmospheric Pressure to Fluorinert. Gain = 0.001.  
Vac = 2.625 kV rms.

	Ch. 2	Ch. 3	Ch. 4	Ch. 5	Ch. 6	Ch. 7	Time	DC, kV	Pressure, mV
			19809	4641	0	0	09:40:03	2.52	8790
			15130	5728	0	0	00:41:40	2.48	8800
			14075	5002	0	0	09:43:17	2.54	8800
			14850	4608	0	0	09:44:54	2.48	8800
Pour in Fluorinert FC-77 →			11058	2188	0	0	09:46:31	2.56	8800
			4	4	0	0	09:48:08	2.52	8800

(b) Gain = 0.100

	Ch. 2	Ch. 3	Ch. 4	Ch. 5	Ch. 6	Ch. 7	Time	DC, kV	Pressure, mV
	2531	4204	0	0	-	-	09:48:47	2.56	8800
	5007	16977	0	0	-	-	09:50:25	2.56	8800
	4934	16549	0	0	-	-	09:52:02	2.54	8800
	5336	16279	0	0	-	-	09:53:39	2.54	8790

(c) Transition from Atmospheric Pressure to Vacuum.  
Vac = 1.2 kV while pumping.

	Ch. 2	Ch. 3	Ch. 4	Ch. 5	Ch. 6	Ch. 7	Time	DC, kV	Pressure, mV
							10:12:00	1.14	8800
			4625	5686	0	0	10:13:36	1.10	7800
			3845	17095	11	0	10:15:14	1.12	7300
			7082	25333	6	0	10:16:52	1.06	6420
			5697	26898	0	0	10:18:30	1.06	4420
			18019	11092	0	0	10:20:07	1.06	3420
			14879	1115	0	0	10:21:44	1.06	2700
			5674	0	0	0	10:23:21	1.08	2300
			5739	1264	0	0	10:24:58	1.08	1600
			480	486	0	0	10:26:35	1.12	240
			0	0	0	0	10:28:13	1.12	180 (-2 mT)

1.4 times the working voltage, where the latter is defined as the maximum instantaneous voltage occurring under normal operation, i.e.,

$$V_{rms}(\text{test}) = 1.4[V_{ac}(\text{peak}) + V_{dc}] \quad (1)$$

In addition, MIL-T-27 indicates that the test voltage be applied for a minimum of 5 sec for quality conformance inspection and 1 min for qualification inspection. The maximum duration is not specified.

Early PDTs of the HV transformer at one manufacturer used both 60-Hz ac test voltage and dc test voltage. The magnitude of the ac test voltage was based on Eq. (1), whereas the dc voltage was arbitrarily set at several times the ac level. The test results in air are given in Table 2. For ac test voltages, CIV occurred at 2 kVrms. At higher test voltages, e.g. at 2.5 kVrms, higher discharge rates and magnitudes were observed. For dc test voltages, CIV occurred at 3 kV, a level consistent with the peak value of the rms CIV. Note that the ac-voltage-associated discharge rates are much higher than the dc-voltage-associated discharge rates. Furthermore, the dc discharge rates decreased rapidly with time. [These differences are consistent with the results reported in studies of ac and dc voltage-excited discharges in a cavity in insulation (Ref. 5).] These dc responses make interpretation of the dc PDT results difficult and therefore unreliable; consequently, dc voltage PDTs of the HV transformer are not recommended.

These investigations also examined the effects of various combinations of ac and dc voltages on CIV and CEV. The results of tests on a HV transformer are given in Tables 3 through 5. First, CIV and CEV were established, using ac voltage only (Table 3). In the first case (Table 4), the ac voltage was increased above the CEV but was kept below the CIV; dc voltage was then added so that  $V_{ac} + V_{dc} > CIV$ , resulting in detectable discharge activity. In the second case, the dc voltage was increased much above the CEV and CIV. No discharge activity above background was monitored. In the third case (Table 5), the dc voltage was increased above CIV but the ac voltage was kept below CEV. Again, no discharge activity was monitored. The ac voltage was then increased above CEV, and discharge activity was monitored again. (These observations are consistent with the results reported in Ref. 6.)

Table 2. PDT Data Showing the Effects of AC and DC Test Voltages. Time Period is 100 sec.

(a) AC PDT of T-2, SN 009 (1-3, 21-22 to 7-8); Gain = 1.000; Test in Air.						
Ch. 1 (Q < 2.5 $\mu$ C)	Ch. 2 (2.5 < Q < 25 $\mu$ C)	Ch. 3 (25 < Q < 250 $\mu$ C)	Ch. 4 (0.25 < Q < 2.5 nC)	Ch. 5 (2.5 < Q < 25 nC)	Time	AC, kV rms
249	0	0	0	-	14:20:21	1.4
430	0	0	0	-	14:21:59	1.4
331	0	0	0	-	14:23:37	
3955	0	0	0	-	14:25:15	1.5
5760	0	0	0	-	14:26:53	1.5
CIV *						
21632	222	6	0	-	14:28:31	2.0
15542	160	0	0	-	14:30:10	2.0
9104	47	0	0	-	14:31:49	2.0
5229	21	0	0	-	14:33:28	2.0
7900	24	0	0	-	14:35:07	2.0
3630	418	0	0	-	14:36:46	2.0
1491	3179	5	0	-	14:38:25	2.0
1102	345	0	0	-	14:40:04	2.0
1414	0	0	0	-	14:41:43	2.0
1426	0	0	0	-	14:43:21	2.0
-31547	28874	28852	974	-	14:44:59	2.5
-41079	31809	35222	4813	-	14:46:39	2.5
-37923	31358	28529	7638	-	14:48:18	2.5
(b) DC PDT of T-2, SN 009 (1-3, 21-22 to 7-8); Gain = 0.100; Test in Air						
-	0	0	0	0	13:54:07	0.00
-	0	0	0	0	13:55:46	0.00
-	0	0	0	0	13:57:24	-1.02
-	0	0	0	0	13:59:02	-1.02
-	0	0	0	0	14:00:40	-1.02
-	0	0	0	0	14:02:18	-2.00
-	0	0	0	0	14:03:56	-2.00
-	0	0	0	0	14:05:34	-2.00
-	10	1	0	0	14:07:12	-3.00
-	1	0	0	0	14:08:51	-3.00
-	0	0	0	0	14:10:29	-3.00
-	43	12	1	0	14:12:07	-4.08
-	0	1	0	0	14:13:47	-4.08

Table 2. PDT Data Showing the Effects of AC and DC Test Voltages. Time Period is 100 sec. (Continued)

(b) DC PDT of TU2, SN 009 (1-3, 21-22 to 7-8); Gain = 0.100; Test In Air (Continued)

Ch. 1 ( $q < 2.5 \mu\text{C}$ )	Ch. 2 ( $2.5 < q < 25 \mu\text{C}$ )	Ch. 3 ( $25 < q < 250 \mu\text{C}$ )	Ch. 4 ( $0.25 < q < 2.5 \text{ mC}$ )	Ch. 5 ( $2.5 < q < 25 \text{ mC}$ )	Time	AC, kV rms	DC, kV
-	1	0	0	0	14:15:26	-	-4.08
-	28	21	0	0	14:17:04	-	-5.04
-	3	1	0	0	14:18:43	-	-5.04
-	0	0	0	0	14:20:22	-	-5.04
-	108	34	0	0	14:22:00	-	-6.08
-	0	3	1	0	14:23:39	-	-6.08
-	0	0	0	0	14:25:19	-	-6.10
-	115	38	1	0	14:26:57	-	-7.04
-	17	1	0	0	14:28:36	-	-7.06
-	10	0	0	0	14:30:15	-	-7.04
-	156	44	1	1	14:31:53	-	-8.12
-	16	4	0	0	14:33:33	-	-8.12
-	17	0	0	0	14:35:12	-	-8.10
-	10	3	0	0	14:36:50	-	-8.10
-	10	3	0	0	14:38:29	-	-8.10
-	6	1	0	0	14:40:08	-	-8.12
-	6	0	0	0	14:41:47	-	-8.10
-	7	1	0	0	14:43:25	-	-8.14
-	3	0	0	0	14:45:04	-	-8.12
-	4	2	0	0	14:46:42	-	-8.10
-	3	0	0	0	14:48:21	-	-8.12
-	3	1	0	0	14:49:59	-	-8.10
-	138	31	5	0	14:51:38	-	-0.02
-	21	0	0	0	14:53:17	-	0.00
-	4	0	0	0	14:54:55	-	0.00
-	5	2	0	0	14:56:33	-	0.00
-	4	1	0	0	14:58:12	-	0.00
-	1	0	0	0	14:59:51	-	0.00
-	3	0	0	0	15:01:29	-	0.00

Table 3. PDT Data Showing AC Voltage Determination of CIV and CEV.  
 T-2/V-2 (1-3, 20-21 to 7-8) in FC-77. Time period is  
 100 sec.

	Ch. 2	Ch. 3	Ch. 4	Ch. 5	Ch. 6	Ch. 7	Time	Temp., °C	Vdc	Vac
	0	0	0	0	0	0	14:22:11	27.8	0	0
	7	0	0	0	0	0	14:24:20	27.8	0	0
	8	0	0	0	0	0	14:25:59	27.8	0	0
	12	0	0	0	0	0	14:27:38	27.8	0	0
	14	0	0	0	0	0	14:29:17	27.8	0	1019
	13	0	0	0	0	0	14:30:58	27.8	0	2010
	10	0	0	0	0	0	14:32:38	27.8	0	2000
	16	0	0	0	0	0	14:34:17	27.8	0	2410
	19	0	0	0	0	0	14:35:56	28.0	0	2410
	16	0	0	0	0	0	14:37:35	27.8	0	2410
	21	0	0	0	0	0	14:39:14	28.0	0	2600
	16	0	0	0	0	0	14:40:53	28.0	0	2600
	18	0	0	0	0	0	14:42:32	28.0	0	2600
CIV →	26205	3355	1	0	0	0	14:44:11	27.8	0	2590
	23233	845	0	0	0	0	14:45:51	27.8	0	2600
	20393	566	0	0	0	0	14:47:31	27.8	0	2600
	6878	110	0	0	0	0	14:49:11	27.8	0	1302
	6780	0	0	0	0	0	14:50:52	27.8	0	1304
	1360	0	0	0	0	0	14:52:31	27.8	0	1231
	217	0	0	0	0	0	14:54:10	28.0	0	1218
	12	0	0	0	0	0	14:55:49	28.0	0	1217
	10	0	0	0	0	0	14:57:28	28.0	0	1217
	10	0	0	0	0	0	14:59:07	27.8	0	1216
	6	9	0	0	0	0	15:00:46	27.8	0	0
	9	0	0	0	0	0	15:02:26	27.8	0	0
	8	0	0	0	0	0	15:04:05	28.0	0	0

Table 4. PDT Data Showing the Effects of AC and DC Test Voltages on CIV and CEV. T-2/V-2 (1-3, 20-21 to 7-8) in FC-77. Time Period is 100 sec.

Ch. 2.	Ch. 3	Ch. 4	Ch. 5	Ch. 6	Ch. 7	Time	Temp., °C	Vdc	Vac
<u>CASE 1</u>									
89	0	0	0	0	0	9:16:03	22.2	0	0
88	0	0	0	0	0	9:17:42	22.4	0	0
94	0	0	0	0	0	9:19:21	22.4	0	2050
98	0	0	0	<u>Vac &lt; CIV</u>		9:21:03	22.4	0	2010
100	0	0	0	0	0	9:22:42	22.4	0	2010
97	0	0	0	0	0	9:24:21	22.4	0	2010
1586	375	2	0	<u>Vac + Vdc &gt; CIV</u>		9:26:00	22.4	-2040	2020
10061	9430	0	0	0	0	9:27:40	22.4	0	2020
1218	1127	0	0	0	0	9:29:20	22.4	0	1232
98	0	0	0	0	0	9:31:01	22.7	0	1233
97	0	0	0	0	0	9:32:40	22.4	0	1231
98	0	0	0	0	0	9:34:19	22.7	0	1233
<u>CASE 2</u>									
94	0	0	0	0	0	10:18:55	23.6	-2440	0
97	0	0	0	0	0	10:20:34	23.6	-2440	0
90	0	0	0	0	0	10:22:13	23.6	-2600	0
90	0	0	0	<u>Vdc &gt; CIV</u>		10:23:52	23.6	-2600	0
85	0	0	0	0	0	10:25:31	23.3	-2600	0
87	0	0	0	0	0	10:27:10	23.6	-2800	0
94	0	0	0	0	0	10:28:49	23.8	-2800	0
90	0	0	0	0	0	10:30:28	23.6	-2840	0
88	0	0	0	0	0	10:32:07	23.6	-3000	0
65	0	0	0	0	0	10:33:46	23.8	-3000	0
32	0	0	0	0	0	10:35:25	23.8	-3000	0
28	0	0	0	0	0	10:37:04	23.8	-3520	0
37	1	0	0	0	0	10:38:43	23.8	-3520	0
34	0	0	0	0	0	10:40:23	23.8	-3520	0
36	0	0	0	0	0	10:42:02	23.8	-4000	0
47	2	0	0	0	0	10:43:41	23.8	-4000	0
49	0	0	0	0	0	10:45:21	23.8	-4000	0

Table 5. PDT Data Showing the Effects of AC and DC Test Voltages on CIV and CEV. T-2/V-2 (1-3, 20-21 to 7-8) in FC-77. Time period is 100 sec.

	Ch. 2	Ch. 3	Ch. 4	Ch. 5	Ch. 6	Ch. 7	Time	Temp., °C	Vdc	Vac
	84	0	0	0	0	0	13:15:10	27.1	0	0
	81	0	0	0	0	0	13:16:49	27.1	0	0
	85	2	0	0	-	-	13:18:28	27.1	0	1018
	89	0	0	0	0	0	13:20:09	27.1	0	1018
	87	0	0	0	0	0	13:21:48	27.1	0	1016
	142	0	0	0	0	0	13:41:36	27.3	-1000	1021
	165	0	0	0	0	0	13:43:15	27.3	-1000	1021
	171	0	0	0	0	0	13:44:54	28.0	-1000	1018
	154	0	0	0	0	0	13:46:34	27.1	-1200	1017
	166	0	0	0	0	0	13:48:13	26.9	-1200	1019
	158	0	0	0	0	0	13:49:52	26.9	-1200	1020
	128	0	Vac < CEV; Vac + Vdc < CIV			0	13:51:31	26.9	-1240	1018
	159	0	0	0	0	0	13:53:10	26.9	-1400	1020
	165	0	0	0	0	0	13:54:49	27.1	-1440	1022
	167	0	0	0	0	0	13:56:28	26.9	-1440	1013
	161	0	0	0	0	0	13:58:07	26.9	-1600	1015
	165	0	0	0	0	0	13:59:46	27.1	-1600	1014
	163	0	0	0	0	0	14:01:25	27.1	-1600	1015
	166	0	0	0	0	0	14:03:04	27.1	-1800	1019
	160	0	0	0	0	0	14:04:43	27.1	-1760	1012
	166	0	0	0	0	0	14:06:22	27.1	-1800	1012
	164	0	0	0	0	0	14:08:01	26.9	-2040	1011
	164	0	0	0	0	0	15:02:35	28.0	-5040	1010
	165	0	0	0	0	0	15:04:14	28.0	-5040	1011
No Corona	165	0	Vac < CEV; Vac + Vdc > CIV				15:05:53	28.2	-5000	1012
	163	0	Vac < CIV; Vac + Vdc > CIV				15:07:32	28.0	-5040	1013
	165	0	0	0	0	0	15:09:11	28.2	-5040	1203
	166	0	0	0	0	0	15:10:50	28.2	-5000	1204
	152	0	0	0	0	0	15:12:30	28.2	-5000	1205
	10178	5	0	0	0	0	15:14:09	28.4	-5040	1388
Corona +	11843	0	0	0	0	0	15:15:49	28.4	-5040	1390
	5800	0	Vac < CIV; Vac + Vdc > CIV				15:17:28	28.4	-5040	1389
	1454	0	0	0	0	0	15:19:07	28.4	-5040	1214
	162	0	0	0	0	0	15:20:46	28.4	-5080	1215
	146	0	0	0	0	0	15:22:25	28.7	-5040	1215
	154	0	0	0	0	0	15:24:04	28.7	-5040	1216
	155	0	0	0	0	0	15:25:43	28.6	-5080	1215
	154	0	0	0	0	0	15:27:22	28.7	-5040	1212
	156	0	0	0	0	0	15:29:01	28.8	-5040	1214
	157	0	0	0	0	0	15:30:40	28.7	-5040	1412
	4076	0	0	0	0	0	15:32:19	29.1	-5080	1413
	3737	0	0	0	0	0	15:33:59	31.0	-5040	1416

A HV transformer acceptance criterion derived from the above study, for transformers exhibiting CIV and CEV below the specified test maximum and operating at Vac and Vdc, was that transformer was judged acceptable for long-term space operations, provided that

$$V_{ac(rms)} + V_{dc} < CIV$$

and

$$V_{ac(rms)} \ll CEV$$

These investigations also examined the effect of test duration on CIV. The results of determining CIV and CEV repeatedly on the same insulation barrier of a HV transformer are schematically shown in Fig. 7. On data such as these, the following general response rules for CIV and delay are based:

1. The CIVs generally decreased with increases in delay time (time at voltage before onset of discharge activity), as indicated in Fig. 8a.
2. For CIVs with no delays (CIVs occurring as the voltage is increased at a constant rate), consecutive measurements show a decrease in CIV, as indicated in Fig. 8b.
3. For CIVs with delays (CIVs occurring after application of constant voltage), consecutive measurements show a decrease in delay time, as indicated in Fig. 8c.
4. In tests on the same insulation barrier, changes from the above variation in CIV and delay time can occur.

The first three rules above are indirectly discussed in Ref. 6.

Partial-discharge (corona) testing of a HV transformer to  $1.5[V_{ac(peak)} + V_{dc}]$  is generally accepted by the manufacturers. A test duration to a minimum of 5 min is recommended, on the basis of the observation of CIV occurring several minutes after application of a constant voltage in numerous tests. The recommendation to test a HV transformer to levels higher than that indicated above is discussed below.

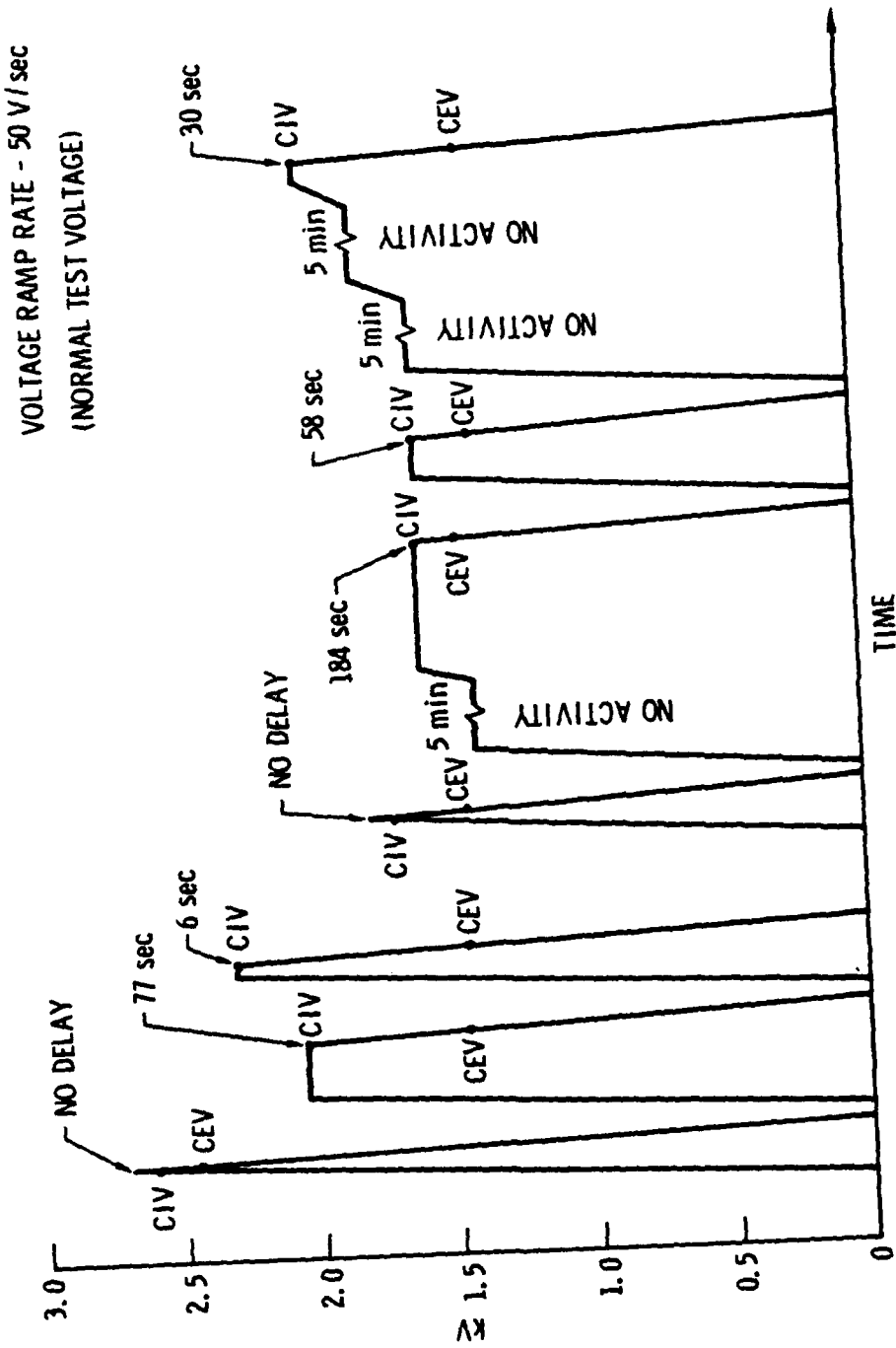


Fig. 7. Representative HV Transformer Test Data Showing CIV, CEV, and Delay in CIV

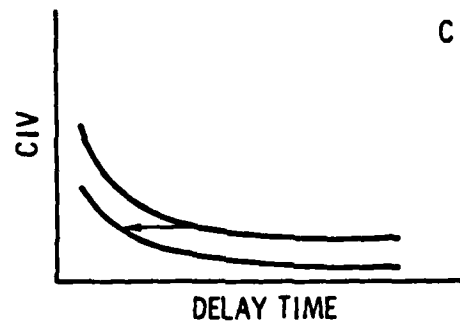
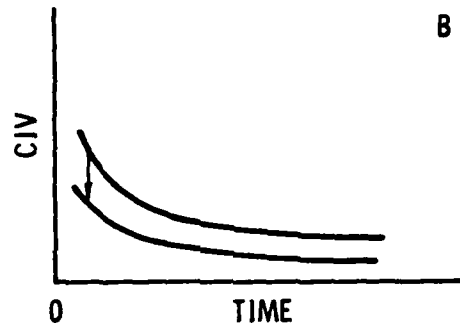
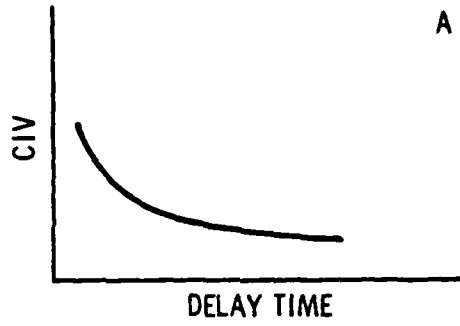


Fig. 8. (a) General Variation of CIV with Delay Time. (b) CIV with No Delay for Same Test Sample. (c) Variation of Delay Time at Constant CIV.

#### IV. PARTIAL-DISCHARGE TESTS AND DESTRUCTIVE PHYSICAL ANALYSIS OF HIGH-VOLTAGE TRANSFORMERS

##### A. PARTIAL-DISCHARGE TESTS OF HIGH-VOLTAGE TRANSFORMERS SN 008 AND SN 016

To determine the effectiveness of the partial-discharge (corona) test described above, which has been generally adopted by the transformer manufacturers, two HV transformers were requested for testing and DPA at Aerospace. These were a HV transformer that had failed the manufacturer's PDT (SN 008) and a HV transformer that had passed (SN 016). These transformers were divider and barrier tested at Aerospace, the former tests using the resistive voltage-divider network designed by the manufacturer. The transformer barrier working voltages, as well as the manufacturer's and Aerospace's barrier test voltages, are given in Table 6. All the voltages given in Table 6 and the following tables are in terms of rms values. For working voltages above 700 V, the manufacturer has used a multiplicative factor of 1.5. For working voltages below 700 V, a larger multiplicative factor has been used as suggested in MIL-T-27. The Aerospace barrier test voltages are 1.33 times higher than those of the manufacturer.

SN 008 was first tested with the divider designed by the manufacturer. CIV was detected at 3600 V, and CEV was noted at 2100 V. These test results are given in Table 7, along with the corresponding effective barrier voltages. SN 008 was then barrier tested to the Aerospace levels given in Table 6. CIV was detected at 900 V and CEV at 600 V in the test of the 10-11 barrier. All other barriers did not show CIV when tested to maximum voltage, as indicated in Table 7.

The defect site in SN 008 appears to be in the 10-11 barrier. This observation is supported by the close agreement between the CIV and CEV obtained by the barrier test and the effective CIV and CEV obtained by the divider test. These test results confirm those of the manufacturer, indicating that SN 008 was a defective transformer.

PREVIOUS PAGE  
IS BLANK



Table 6. Working Voltages and Test Voltages for Two HV Transformers

Barrier	Vac	Vdc	Vac + Vdc	1.5(Vac + Vdc)	Manuf.	Aerospace
8-9	275	733	1008	1512	1700	2200
10-11	0	1100	1100	1650	1700	2200
12-13	93	457	550	825	1200	1600
14-15	0	364	364	546	1200	1600
16-17	121	486	607	910	1200	1600
18-19	0	607	607	<u>910</u>	1200	1600
				6350		

Table 7. PDT Results for HV Transformer SN 008

Barrier	Divider Test		Barrier Test	
	CIV = 3600 V	CEV = 2100 V	CIV	CEV
8-9	706	412	---	---
10-11	1055	615	900	600
12-13	439	256	---	---
14-15	349	204	---	---
16-17	468	273	---	---
18-19	583	340	---	---

SN 016 also was first tested with the divider method. CIV was detected at 5500 V. CEV was noted at 2800 V. The corresponding effective barrier voltages are given in Table 8. A barrier test of SN 016 showed CIV at 2000 V and CEV at 1600 V for the 8-9 barrier, and CIV at 2200 V and CEV at 1600 V for the 10-11 barrier, as given in Table 8.

The above Aerospace results do not agree with those of the manufacturer, which indicated the absence of corona (no CIV) in the divider test as well as in the barrier test. Disagreement in the barrier test results is understandable if the manufacturer tested to only the levels shown in Table 6, i.e., to voltages <1700 V. It is suspected that the divider test results do not agree because the manufacturer tested to only 4500 V (as recommended in one of its internal memoranda) and not to 6000 V [as required to meet the 1.5 (Vac + Vdc) condition indicated in Table 6]. Therefore, the manufacturer could have detected CIV indicating defects in SN 016, as confirmed by the subsequent DPA, if it had tested to higher voltages.

A discrepancy noted in the results given in Table 8 is that the barrier voltages for CIV and CEV are much higher than the corresponding effective barrier voltages applied during divider testing. This difference for the 8-9 barrier is almost a factor of 2 for CIV (2000 V compared to 1078 V) and almost a factor of 3 for CEV (1600 V compared to 548 V). These results suggest that the two sets of CIVs and CEVs correspond to different defects. This possibility is discussed below.

B. DESTRUCTIVE PHYSICAL ANALYSIS OF HIGH-VOLTAGE TRANSFORMERS  
SN 008 AND SN 016

Destructive physical analysis was performed on both transformers after completion of PDT. The results of primary interest showing the cross section of the toroidal transformers are given in Fig. 9 for SN 008 and Fig. 10 for SN 016. In both units, crack defects were found only in the section inside the toroidal core. A cross section of this area is given in Fig. 11 for SN 008 and in Fig. 12 for SN 016.

As predicted by the PDT results given in Table 7, HV defects are found in the 10-11 barrier of SN 008. However, although these defects are the largest

Table 8. PDT Results for HV Transformer SN 016

Barrier	Divider Test		Barrier Test	
	CIV = 5500 V	CEV = 2800 V	CIV	CEV
8-9	1078	548	2000	1600
10-11	1612	821	2200	1600
12-13	671	342	---	---
14-15	533	272	---	---
16-17	715	764	---	---
18-19	891	454	---	---

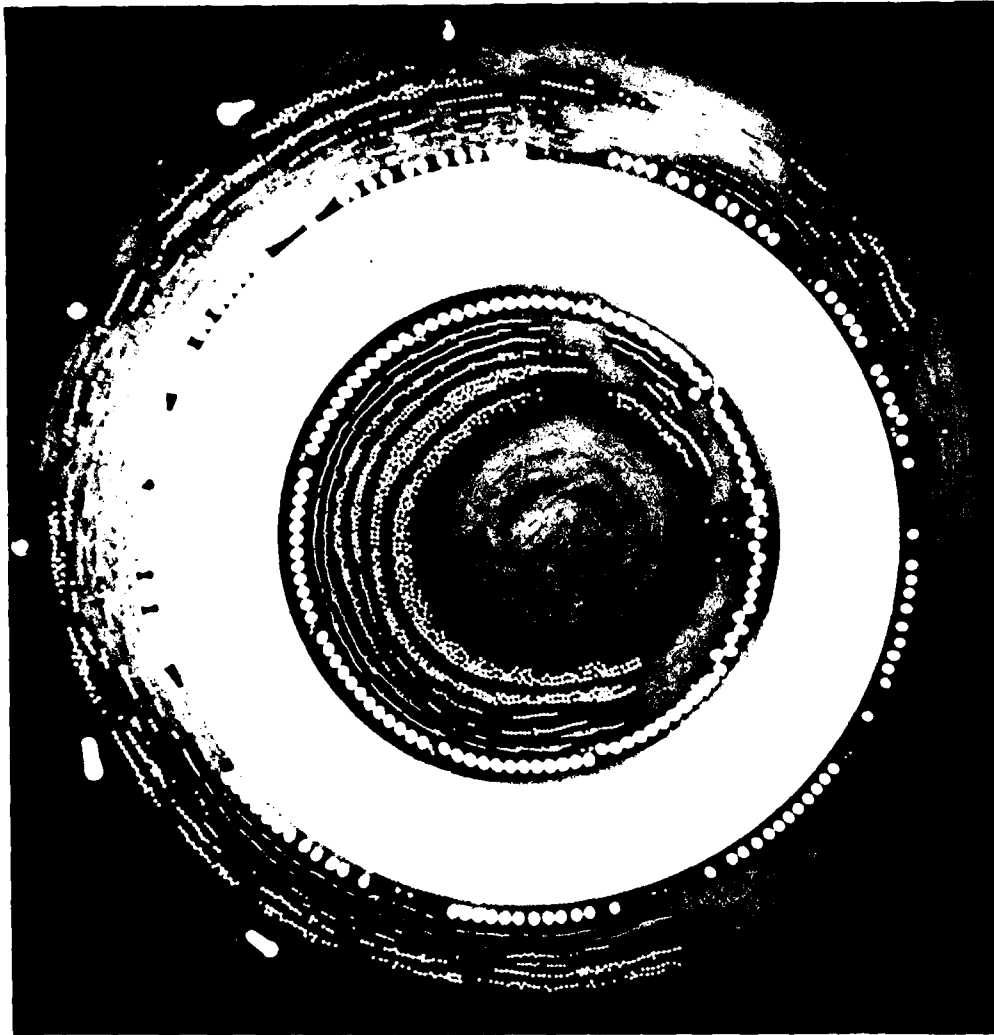


Fig. 9. Cross Section of HV Transformer SN 008

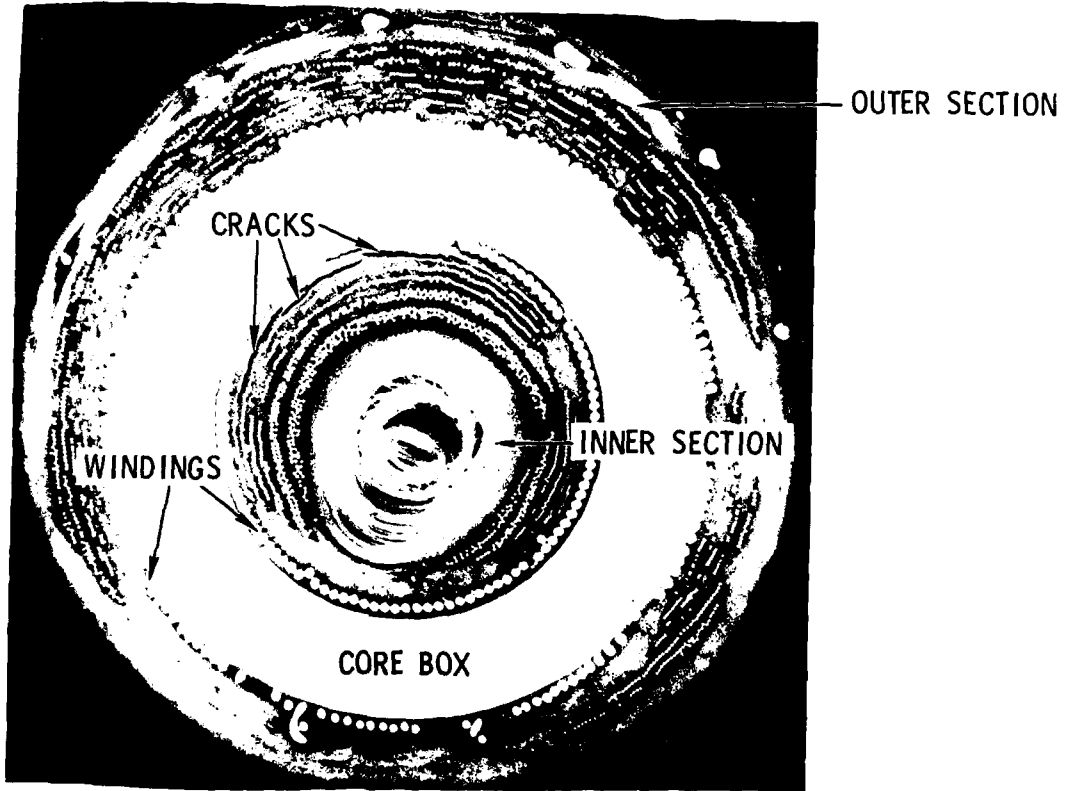


Fig. 10. Cross Section of HV Transformer SN 016

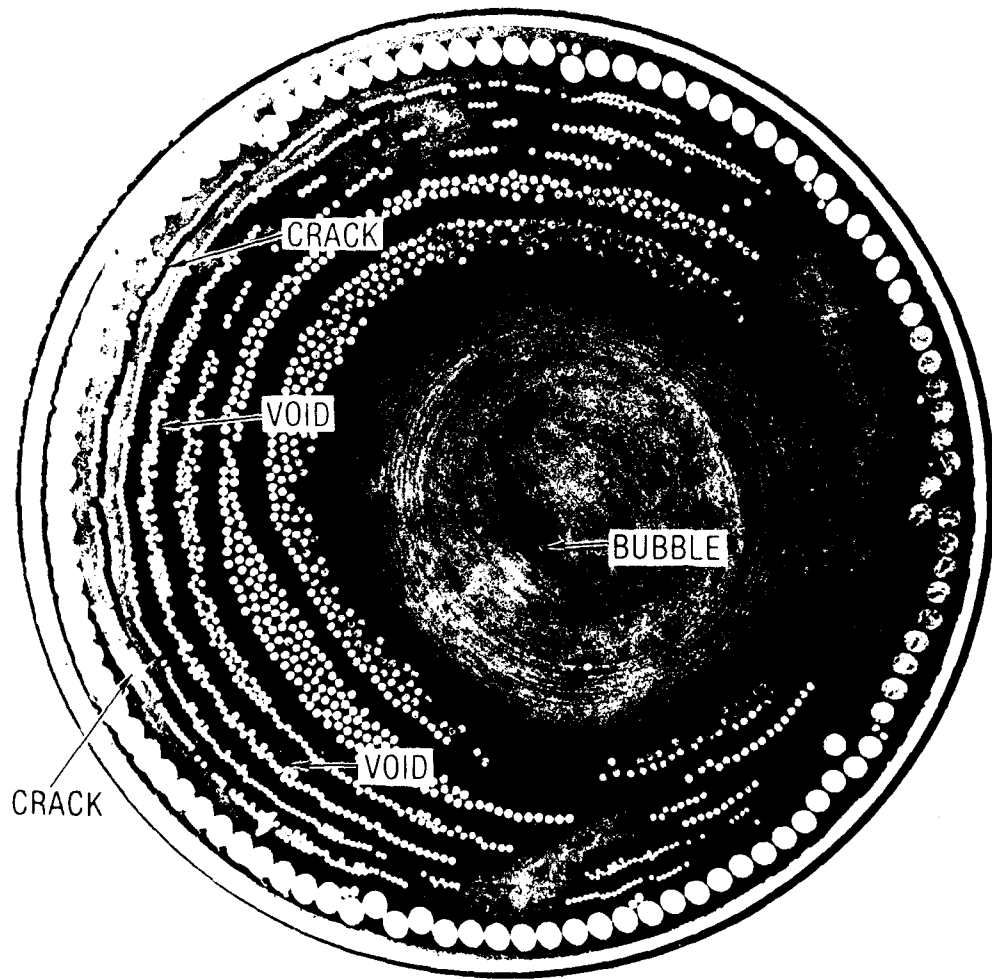


Fig. 11. Core Cross Section of SN 008, Showing Locations of Cracks and Voids

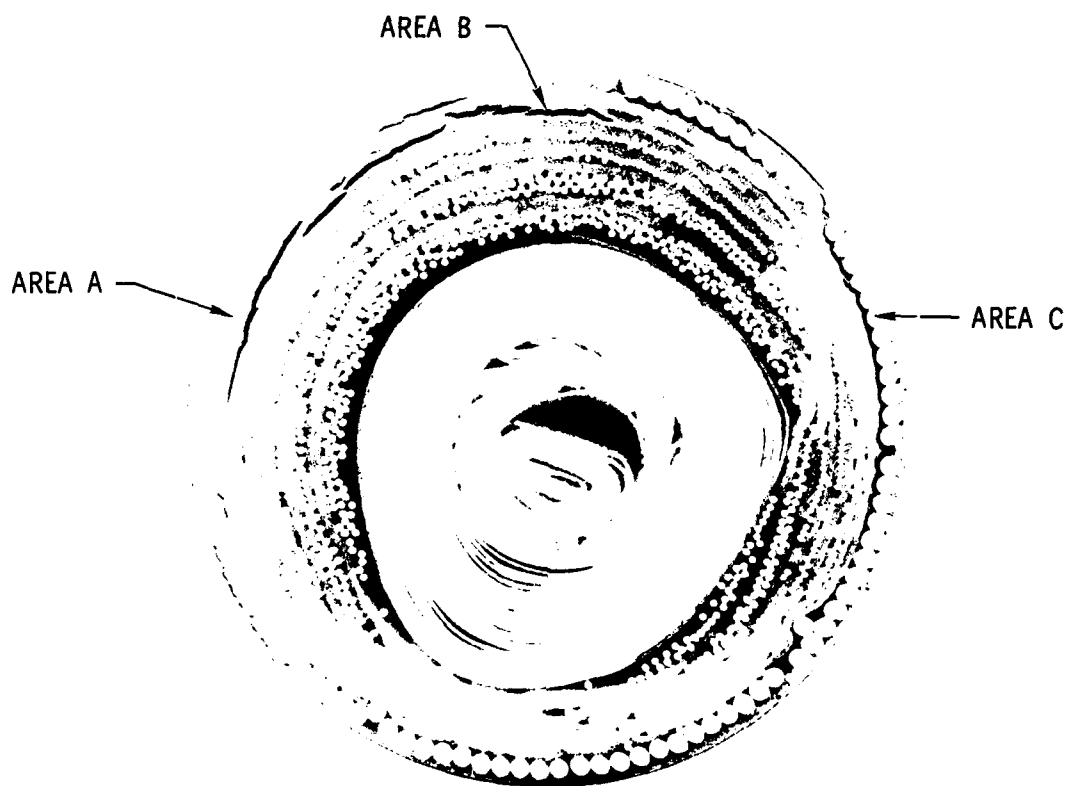


Fig. 12. Core Cross Section of SN 016, Showing Locations of Cracks and Voids

ones found, other defects are noted in Fig. 11. These were not detected by PDT, probably because the tests were not performed to high enough voltages. The crack defects in barriers 8-9 and 10-11 of SN 016 are predicted by the barrier test results in Table 8. Cracks occur not only in areas where the barriers are defined by adjacent windings, such as areas A and B in Fig. 12, but also in areas where the barrier is not well defined, such as area C. As indicated above, the divider test results do not agree with the barrier test results, suggesting that the latter results may be associated with defects in these poorly defined areas. This possibility is examined by means of a simple model of discharges occurring in a planar gap under electrical stress.

## V. MODEL OF DISCHARGES OCCURRING IN A PLANAR GAP

Electrical breakdown (gaseous ionization) across a planar gap between metal or dielectric electrodes is described by the Paschen curve (Ref. 7). This curve, as usually presented, gives the voltage required for gap breakdown as a function of the product of gap spacing and gas pressure. However, if the gas pressure is specified, breakdown voltage is just a function of gap spacing. The Paschen curve in this form, determined experimentally by Perkins (Ref. 8) for a planar electrode configuration at atmospheric pressure, is given in Fig. 13. Breakdown voltage is given in kV (rms) and the gap (crack) spacing is in mils. Note that at atmospheric pressure, the minimum breakdown voltage occurs near 1 mil gap spacing. This curve is affected by both a change in gas specie and a change in gas pressure. The curve in Fig. 13 shifts to the right as the pressure is reduced.

For the calculations given in this report, the Paschen curve used is that for atmospheric pressure. The only justification to date for this selection is that, with its use, correlation between PDT results and those of DPA appears to be possible, as shown in the cases given below. (In other cases where correlation is not possible with this selection, the Paschen curve at other pressures should be considered. To provide direct justification for the use of a particular Paschen curve, investigations of gas pressure in closed cavities in various polymer encapsulants, including Epon 825, are being performed.)

The model assumed for discharges occurring in a planar gap in an encapsulated transformer is shown in Fig. 14. A crack of width  $d_1$  occurs in the insulation barrier between a set of windings. This barrier consists of polymat-filled epoxy with a dielectric constant of  $K = 4.5$ . During operation or test, an ac voltage difference  $V$  is applied across the barrier of width  $d$ . The voltage appearing across the crack  $V_1$ , determined as indicated in Fig. 14, is given by

$$V_1 = \left( \frac{1}{(1 - 1/K) + d/Kd_1} \right) V \quad (2)$$

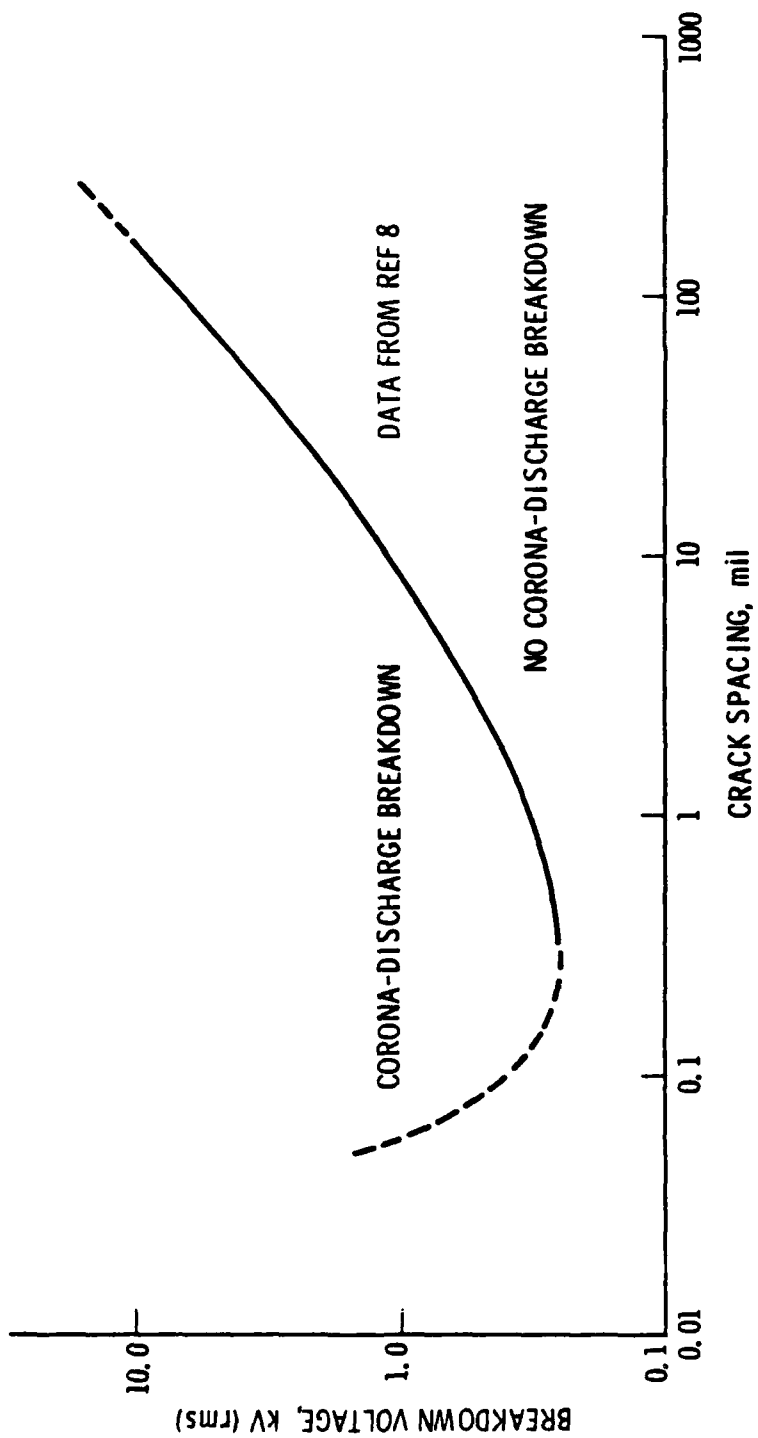


Fig. 13. The Paschen Curve at Atmospheric Pressure

V - VOLTAGE APPLIED ACROSS WINDING TERMINALS

V<sub>1</sub> - VOLTAGE ACROSS CRACK

V<sub>2</sub> - VOLTAGE ACROSS POTTING

d<sub>1</sub> - CRACK WIDTH

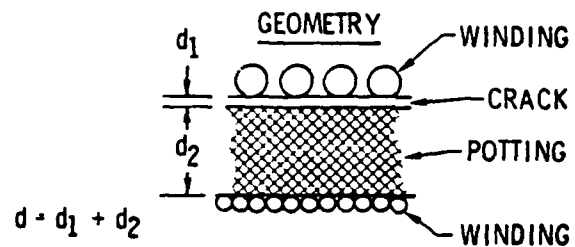
d<sub>2</sub> - POTTING WIDTH

C<sub>1</sub> - CRACK CAPACITANCE

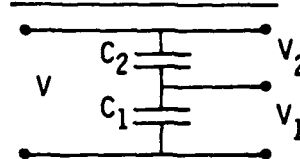
C<sub>2</sub> - POTTING CAPACITANCE

K - DIELECTRIC CONSTANT OF POTTING = 4.5

d - ELECTRODE (WINDING) SEPARATION.



EQUIVALENT CIRCUIT



$$V_1 = \frac{1}{\left(1 - \frac{1}{K}\right) + \frac{d}{K d_1}} V$$

$$V_1 = \frac{C_2}{C_1 + C_2} V = \frac{K/d_2}{1/d_1 + K/d_2} V$$

Fig. 14. Model for Determination of Crack Voltage

If the voltage  $V_1$  exceeds the breakdown voltage given by the Paschen curve, discharges will occur in the crack. These discharges are capacitively coupled to the transformer windings, and the windings are monitored for discharges by the PDT system.

## VI. CORRELATION OF RESULTS OF PARTIAL-DISCHARGE TESTS AND DESTRUCTIVE PHYSICAL ANALYSIS

### A. TRANSFORMER SN 008

In Fig. 11, the barrier and crack widths can be estimated by comparing them with the diameters of the wires of the various windings. Cracks are noted in several places in the 10-11 barrier; here the barrier widths range from 15 to 20 mils and the crack widths range from 2 to 5 mils. To determine whether discharges in SN 008 are described by the simple model proposed above, the crack voltage  $V_1$  was computed as a function of crack spacing  $d_1$  with the parameters (1) barrier spacing  $d = 15$  to 25 mils (from DPA) and (2) barrier voltage  $V = 900$  to 1050 V (from PDT). The plot of  $V_1$  for the maximum-stress case ( $d = 15$  mils and  $V = 1050$  V) gives the curve superimposed on the Paschen curve in Fig. 15.  $V_1$  intersects the breakdown curve at crack spacings ranging from 2 to 5 mils, indicating the possibilities of discharges for a combination of parameter values obtained from PDT and DPA. The simple analytical model proposed appears to be able to correlate the results of PDT and DPA.

### B. TRANSFORMER SN 016

In Fig. 12, cracks are observed in several locations: in the 8-9 barrier, in the 10-11 barrier, and on one side of the 1-8 primary winding. Note that the barriers containing a crack along the primary winding (1-8) in some locations are bounded not by the first secondary winding (9-10), but by the second secondary winding (11-12) or the fifth secondary winding (17-18). This observation may explain the anomaly noted above.

The barrier configuration described above is schematically represented in Fig. 16, with the winding voltages indicated for an applied divider voltage of 5500 V. The barrier widths are estimated from Fig. 12. The following three barriers are examined by means of the simple model for CIV proposed above: barrier 8-9 with 1078 V applied, barrier 8-11 with 2690 V applied, and barrier 8-17 with 4110 V applied. The calculation of crack voltage  $V_1$ , by means of the values of barrier width and barrier voltage given in Fig. 16, gives the curves shown in Fig. 17. The  $V_1$  curve for the 8-9 barrier falls below the

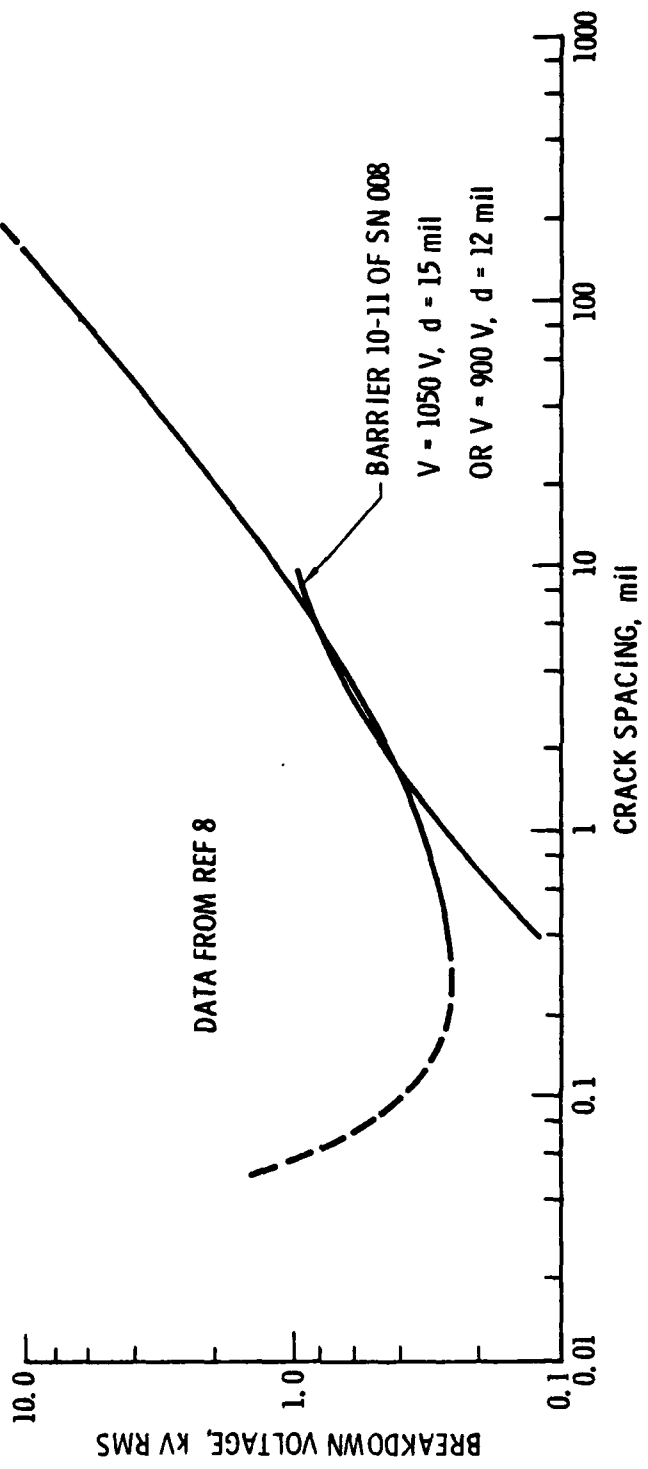


Fig. 15. Conditions for CIV in HV Transformer SN 008

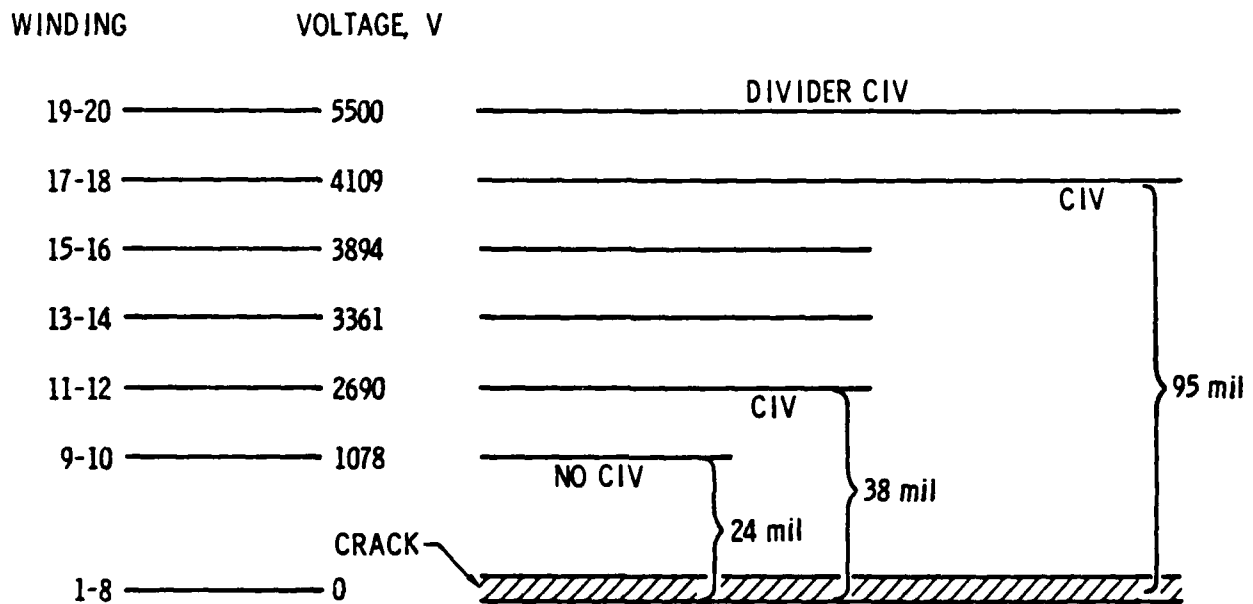


Fig. 16. Resistive Divider Partial-Discharge Test of HV Transformer  
SN 016

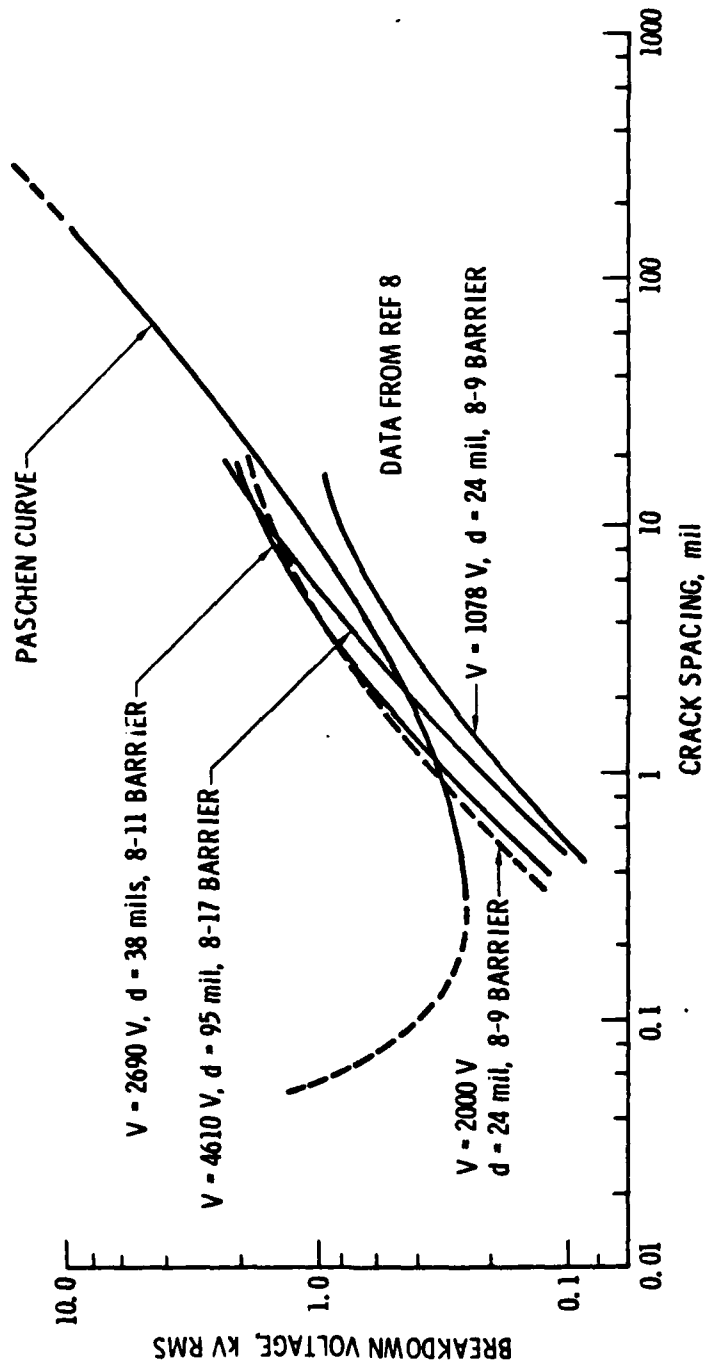


Fig. 17. Conditions for CIV in HV Transformer SN 016

breakdown curve, indicating there is no CIV. However, the V<sub>1</sub> curves for the 8-11 and the 8-17 barriers intersect the breakdown curve at 1.2 and 2.3 mils, respectively, indicating there is CIV in cracks with spacing above these values. As observed in Fig. 12, the cracks associated with the above barriers are certainly greater than 2.3 mils in width. Therefore, under the partial-discharge divider test, discharges can occur in these cracks.

The PDT results using the barrier method give CIV = 2000 V for the 8-9 barrier. The V<sub>1</sub> curve computed for V = 2000 V and d = 24 mils, also shown in Fig. 17, indicates breakdown in cracks with spacing above 1 mil. Because the observed crack spacing is above this value, discharging in this crack is possible, which is consistent with the PDT results.

The above analysis indicates that in the PDT using the divider method, the discharges monitored occurred in the 8-11 and the 8-17 barriers; however, in the PDT that uses the barrier method, the discharges occurred in the 8-9 barrier, explaining the anomaly noted in Table 8.

### C. PDT/DPA ANOMALIES

In a PDT of another HV transformer, CIV was detected with the divider test but not with the barrier test. Subsequent DPA of this transformer showed no defects in any of the barriers. However, several large voids were noted in the core encapsulant outside the barriers. The only plausible explanation for this anomaly is that the discharges observed in CIV occurred in these external voids, the electrical stress being applied between the outer winding of the transformer at high voltage and the ground plane on which the transformer was placed. The voltage was sufficiently high for CIV in the divider test but not in the barrier test.

Another anomaly noted in the PDTs of SN 008, SN 016, and other HV transformers is that small voids revealed by DPA were not detected. One reason for this anomaly may be that these small voids are somewhat spherical in shape, and the mean voltages developed across these voids are much less than those across comparable one-dimensional cracks. For example, the voltage across a small crack is  $V_1 = K(d_1/d)V$ , for  $Kd_1 \ll d$  (see Fig. 14), and the voltage across a spherical void is  $V_1 = \frac{3K}{1+2K} (d_1/d)V$ , where  $d_1$  in the latter

is the diameter of the void. For  $K = 4.5$ , the dielectric constant of the transformer insulation, the voltage across the spherical void is only 27% of the voltage across a comparable crack. This relatively lower voltage may be too low for discharge breakdown, consequently making the void undetectable by the PDT technique.

Another reason for this anomaly may be that discharges occurring in these small voids are too low in magnitude to be detected by the presently used PDT system. An estimate of the magnitude of the discharges in these voids, based on the model given in the Appendix, is given by the expression  $q = C_2 V_1$ , where  $q$  is the discharge magnitude,  $C_2 = K\epsilon_0 A/d_2$  is the capacitance of the encapsulant in series with the void, and  $V_1$  is the void voltage. For voids with discharge area below  $100 \text{ mil}^2$ , with  $d_2 = 30 \text{ mil}$  and  $V_1 = 300 \text{ V}$ ,  $q$  is below  $1 \text{ pC}$  (as indicated in the Appendix). One picocoulomb ( $1 \text{ pC}$ ) is the nominal sensitivity of the present PDT system. Therefore, it appears possible that discharges in small voids are just too low in magnitude to be detected.

Most PDTs of HV transformers were performed to only nominal test voltage levels, i.e., to 1.5 to 2.0 times the operating (working) voltage levels. The correlation of PDT and DPA results generally indicates that significant defects found in some barriers were not detected with partial-discharge testing. To detect these defects, tests to four times operating voltage were examined as described below.

## VII. PARTIAL-DISCHARGE TESTS OF HIGH-VOLTAGE TRANSFORMERS TO EXTRA-HIGH LEVELS

### A. PDT REFERENCE VOLTAGE

The partial-discharge test reference voltages for the HV transformers examined in the preceding sections, based on MIL-T-27 and on the manufacturer's test specifications, are given in Table 9. Note that the working voltage defined by the manufacturer is smaller by a factor of  $1/\sqrt{2}$  than that defined by MIL-T-27. However, the former will be accepted as the reference so that direct comparisons can be made between the test results obtained by Aerospace and those by the manufacturer. The effective divider voltages given are those based on an assembled resistive divider network designed to produce the required voltage distribution. Test voltages at four times the reference are given in Table 10. (The divider voltage distribution given in Table 10 is different from that shown in Tables 7 and 8 because the latter, computed by the manufacturer, were found to be incorrect. This erroneous distribution, however, does not negate the test results or conclusions given above.)

### B. PDT OF SN 010 AT FOUR TIMES OPERATING VOLTAGE

SN 010, another defective HV transformer, was partial-discharge tested to four times the operating (reference) voltage. The results were similar to those for SN 016. Barriers 10-11, 12-13, and 14-15 showed CIVs in the barrier test. However, these CIVs were higher than the corresponding effective CIVs applied in the divider test. DPA of SN 010 revealed not only small cracks and voids in the 10-11, 12-13, and 14-15 barriers, but also large voids in poorly defined barrier areas in the internal core section of the transformer. The higher CIVs observed in the barrier test appear to be associated with the defects in the well-defined barriers, and the lower effective CIVs appear to be associated with the large cavities.

Table 9. PDT Reference Voltages

Barrier	MIL-T-27 <sup>a</sup> 1.5(Vac + Vdc)	Manufacturer <sup>b</sup> 1.5(Vac + Vdc)/√2	Effective Divider Voltage
8-9	1512	1069	1075
10-11	1650	1167	1161
12-13	825	583	587
14-15	546	386	387
16-17	910	644	645
18-19	<u>910</u>	<u>644</u>	<u>645</u>
	6353	4493	4500

<sup>a</sup>The factor 1.5 is used, rather than the 1.4 indicated in MIL-T-27.

<sup>b</sup>The factor 1/√2 was introduced by the manufacturer.

Table 10. PDT Voltages at Four Times the Reference Voltages

Barrier	Reference Voltage $1.5(V_{ac} + V_{dc})/\sqrt{2}$	4× Barrier Voltage	1.5× Divider Voltage	4× Divider Voltage
8-9	1069	3200	1075	2866
10-11	1167	3200	1161	3096
12-13	583	1600	587	1567
14-15	386	1100	387	1032
16-17	644	1700	645	1720
18-19	644	1700	645	1720

### C. PDT OF DEFECT-FREE HV TRANSFORMERS

The HV transformer SN EQM 7T, one of four qualification transformers, was partial-discharge tested to four times the operating voltages with the applied voltages indicated in Table 10. The divider test results indicated by the strip-chart record are shown in Fig. 18. Divider PDTs were conducted at two times (6 kV), three times (9 kV), and four times (12 kV) operating voltages. Transient activity, noted during tests at 9 and 12 kV, was shown to be associated with the test arrangement and not with the transformer by removing the transformer and repeating the tests to 4x voltages. SN EQM 7T passed both the barrier and divider tests, indicating that the transformer was free of HV defects. This conclusion was confirmed by the subsequent DPA.

Another HV transformer, fabricated by a different manufacturer and similar in design and material but different in winding-voltage distribution, was also tested to four times operating voltage. This transformer was identified as a flight backup unit that had been built under improved processing procedures and tested to two times operating voltage by the manufacturer (Ref. 9). At Aerospace, this unit also passed both the barrier and the divider test at four times operating voltage. Performance of the latter test required 12.7 kV across the appropriately designed divider network. DPA was not performed on this unit.

### D. CONCERNS REGARDING PDT TO FOUR TIMES OPERATING VOLTAGE

The primary concern expressed about performing PDTs to four times operating voltage is that tests to this level will initiate HV defects or activate latent defects in the transformer insulation. However, this concern is groundless because there is no evidence, from either the results of DPA or any other source, that this action is occurring. PDT to four times operating voltage levels is conducted for only short periods of time and at relatively low electrical stress levels. Test to the levels indicated in Table 10 show a maximum stress of 215 V/mil, which corresponds to a minimum barrier thickness of 15 mil. For these stress levels and barrier thicknesses, the margin against initiating any degrading effect is considered adequate. However, because of reduced margins, testing to levels beyond four times operating voltage is not recommended.

DIVIDER PDT OF S/NEQM 7T

VOLTAGE DIVIDER

TEST VOLTAGE KV

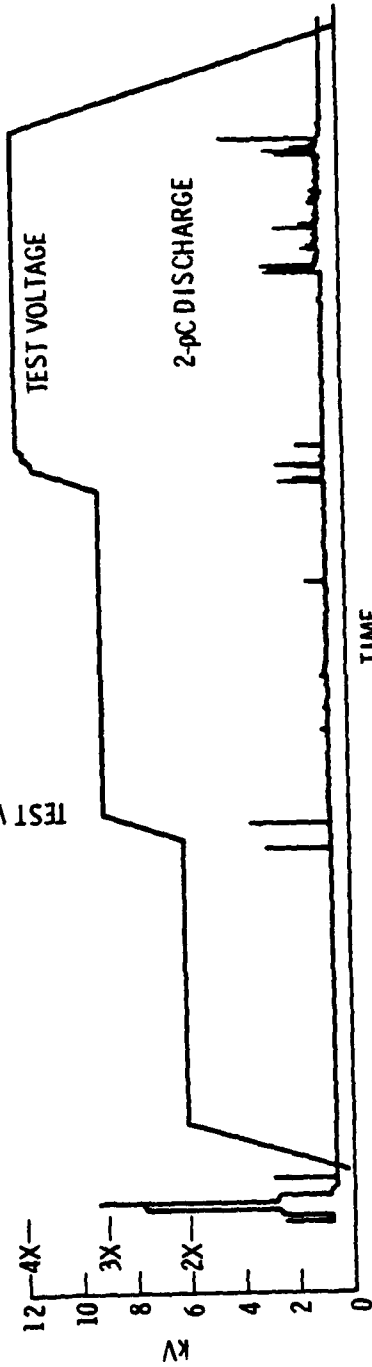


Fig. 18. Strip Chart Recording of Partial-Discharge Test of HV Transformer SN EQM 7T

## VIII. CONCLUSIONS

The partial-discharge (corona) test is the most effective test for screening HV transformers for HV defects. This test should be conducted in a dielectric fluid (FC 77), even though the transformer is expected to see long-term service in vacuum. PDTs should be performed with the divider method rather than the barrier method, because the former simulates more closely the operating voltage distribution, requires less time to apply, and has been able to detect defects occurring at lower stress levels which were undetectable by the barrier method. The pass/fail criterion should be the absence of discharge activity at a detection sensitivity of 1 picocoulomb.

The parameter measured in partial-discharge testing is the corona inception voltage (CIV). A simple analytical model based on gas breakdown in a planar crack can be constructed to describe this CIV phenomenon. This model provides a means to determine if partial-discharge testing performed to a prescribed voltage level is effective in detecting defects of a certain size in a particular transformer configuration.

Partial-discharge test screening of HV transformers is conducted for two reasons: (1) to detect incipient-level defects in these units and/or (2) if these defects are present, to establish that partial discharges will not occur in these defects at operating voltages with an adequate margin of safety. The latter objective is easily achieved by partial-discharge testing to only 1.5 times operating voltage. Testing to this level will provide some margin in the near term which may compensate for possible future degradation of the defects and for the difference between the test stress (60-Hz sine wave) and the operating stress (10 to 20-kHz square wave). However, testing only to this level can also allow significant defects to escape detection, as seen in the examples described above. Therefore, to detect HV defects in a transformer with optimum certainty, testing at four times operating voltage is recommended. Partial-discharge (corona) testing at this level is not prohibited by MIL-T-27. In fact, for transformers designed to operate at pressures below atmospheric, MIL-T-27 indicates that the use of a higher test-voltage magnitude is an option of the supplier.

## REFERENCES

1. E. R. Bunker, J. R. Arnett, and K. H. Li, "Manufacturing Methods and Technology for Electromagnetic Components, Vols. I and II," Hughes Aircraft Co., Aerospace Group, Report No. FR-80-76-1254R, HAC Ref. No. 8712 (December 1980).
2. MIL-T-27, "General Specifications for Transformers and Inductors (Audio, Power, and High-Power Pulse)" (15 April 1974).
3. F. Hai and K. W. Paschen, "DC Partial-Discharge/Environmental Test Screening of Space TWTs," Intersociety Energy Conversion Engineering Conference (21-26 August 1983), Orlando, Fla., Conference Proceedings of the 18th IECEC, Vol. 5, 2216-2222.
4. "Standard Methods for Detection and Measurement of Discharge (Corona) Pulses in Evaluation of Insulation Systems," ASTM D1868-73.
5. R. J. Densley, "Partial Discharge under Direct-Voltage Conditions," Ch. 11 in Engineering Dielectrics, Vol. 1: Corona Measurement and Interpretation, ASTM 669, eds. R. Bartnikas and E. J. McMahon (1979).
6. H. Feibus, "Corona in Solid-Insulation Systems," IEEE Trans. El. Insul., Vol. EI-5, No. 3 (September 1970), 72.
7. J. D. Cobine, Gaseous Conductors (Dover Publications, Inc., New York, 1958).
8. J. R. Perkins, "High-Voltage Wiring and Connector Systems," Ch. 6 in Handbook of Wiring, Cabling, and Interconnecting for Electronics, ed. C. A. Harper (McGraw-Hill Book Co., New York, 1972).
9. P. H. Fowler, D. A. Brent, and G. J. Sidio, "Predicted and Actual High-Voltage Failure - A Case Study," Conference Proceedings of the 18th IECEC, Orlando, Fla. (24 August 1983).

PREVIOUS PAGE  
IS BLANK 

## APPENDIX: A MODEL FOR ESTIMATING DISCHARGE MAGNITUDES

The model used to estimate the magnitude of the discharges in the cracks of a transformer is an extension of the model described in Fig. 14. This model is expanded to include the part of the winding barrier without the cracks, as indicated in Fig. A-1. The capacitances and voltages are as indicated, with  $C_s$  = capacitance of the system and  $V_s$  = voltage of the system at discharge. The discharge magnitude,  $q = C_s V_s$ , is that measured across the transformer winding. Furthermore, for planar geometry where the capacitance  $C = K\epsilon_0 A/d$ ,  $K$  is the dielectric constant of the encapsulant,  $\epsilon_0$  is the permittivity of space ( $8.85 \times 10^{-12}$  F/M),  $A$  is the area, and  $d$  is the spacing, the discharge magnitude reduces to  $q = C_2 V_1$ .  $C_2$  is the capacitance of the encapsulant in series with the crack, and  $V_1$  is the crack voltage.  $C \gg C_2$  (i.e., the lateral area of the crack-free barrier is much larger than that of the crack) and  $C_1 \gg C_2$  (i.e., the crack width is much smaller than the barrier width) have been assumed.

For a numerical estimate of the discharge magnitude, the following is assumed:

$$q = C_2 V_1 = \left( \frac{K\epsilon_0 A}{d_2} \right) V_1$$

where

$$K = 4.5 \text{ (dielectric constant of the filled epoxy)}$$

$$\epsilon_0 = 8.85 \times 10^{-12} \text{ F/M}$$

$$d_2 = 30 \text{ mils} = 7.62 \times 10^{-4} \text{ M}$$

$$V_1 = 300 \text{ V (breakdown minimum)}$$

For these values,  $q = 1.57 \times 10^{-5}$  A (in coulombs, and where  $A$  is the effective area). This effective area is assumed to be equal to one-fourth the actual area. For an effective area of  $100 \text{ mil}^2$  ( $6.45 \times 10^{-8} \text{ M}^2$ ), the discharge

$C_1$  - CRACK CAPACITANCE

$C_2$  - SERIES POTTING CAPACITANCE

$C$  - PARALLEL POTTING CAPACITANCE

$C_S$  - SYSTEM CAPACITANCE

$$C_S = C + \frac{C_1 C_2}{C_1 + C_2}$$

$V_1$  - CRACK VOLTAGE AT DISCHARGE

$V_S$  - V - SYSTEM VOLTAGE AT DISCHARGE

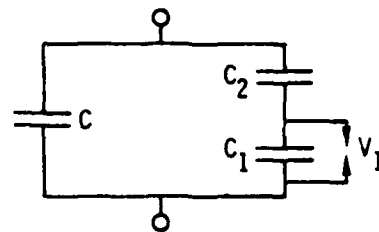
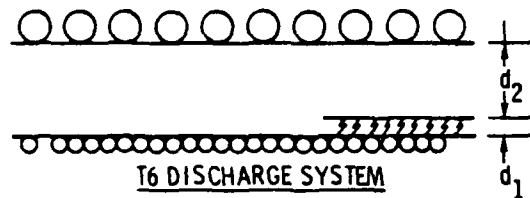
$$V_S = \frac{C_2}{C + C_2} V_1$$

$q$  - MEASURED PARTIAL-DISCHARGE MAGNITUDE

$$q = C_S V_S$$

$$= \left( C + \frac{C_1 C_2}{C_1 + C_2} \right) \left( \frac{C_2}{C + C_2} \right) V_1$$

$$q \approx C_2 V_1 \quad \text{FOR } C \gg C_2 \text{ AND } C_1 \gg C_2$$



EQUIVALENT CIRCUIT

FOR PARALLEL GEOMETRY

$$C_2 = K \epsilon_0 \frac{A}{d_2}$$

$$K = 4.5$$

$$\epsilon_0 = 8.85 \times 10^{-12} \text{ F/M}$$

$A$  - CRACK CROSS-SECTION AREA

Fig. A-1. Determination of Partial-Discharge Magnitude

magnitude is  $1 \times 10^{-12}$  coulomb (1 pC). For larger effective areas, corresponding to extensive cracks, the discharge magnitudes are larger. These large-magnitude discharges are easily detectable by the PDT system at the transformer manufacturer or at Aerospace. However, discharges of magnitude below 1 pC are probably undetectable with these systems.

## LABORATORY OPERATIONS

The Laboratory Operations of The Aerospace Corporation is conducting experimental and theoretical investigations necessary for the evaluation and application of scientific advances to new military space systems. Versatility and flexibility have been developed to a high degree by the laboratory personnel in dealing with the many problems encountered in the nation's rapidly developing space systems. Expertise in the latest scientific developments is vital to the accomplishment of tasks related to these problems. The laboratories that contribute to this research are:

Aerophysics Laboratory: Launch vehicle and reentry fluid mechanics, heat transfer and flight dynamics; chemical and electric propulsion, propellant chemistry, chemical dynamics, environmental chemistry, trace detection; spacecraft structural mechanics, contamination, thermal and structural control; high temperature thermomechanics, gas kinetics and radiation; cw and pulsed chemical and excimer laser development including chemical kinetics, spectroscopy, optical resonators, beam control, atmospheric propagation, laser effects and countermeasures.

Chemistry and Physics Laboratory: Atmospheric chemical reactions, atmospheric optics, light scattering, state-specific chemical reactions and radiative signatures of missile plumes, sensor out-of-field-of-view rejection, applied laser spectroscopy, laser chemistry, laser optoelectronics, solar cell physics, battery electrochemistry, space vacuum and radiation effects on materials, lubrication and surface phenomena, thermionic emission, photosensitive materials and infrared detectors, atomic frequency standards, and environmental chemistry.

Computer Science Laboratory: Program verification, program translation, performance-sensitive system design, distributed architectures for spaceborne computers, fault-tolerant computer systems, artificial intelligence, microelectronics applications, communication protocols, and computer security.

Electronics Research Laboratory: Microelectronics, solid-state device physics, compound semiconductors, radiation hardening; electro-optics, quantum electronics, solid-state lasers, optical propagation and communications; microwave semiconductor devices, microwave/millimeter wave measurements, diagnostics and radiometry, microwave/millimeter wave thermionic devices; atomic time and frequency standards; antennas, RF systems, electromagnetic propagation phenomena, space communication systems.

Materials Sciences Laboratory: Development of new materials: metals, alloys, ceramics, polymers and their composites, and new forms of carbon; non-destructive evaluation, component failure analysis and reliability; fracture mechanics and stress corrosion; analysis and evaluation of materials at cryogenic and elevated temperatures as well as in space and enemy-induced environments.

Space Sciences Laboratory: Magnetospheric, auroral and cosmic ray physics, wave-particle interactions, magnetospheric plasma waves; atmospheric and ionospheric physics, density and composition of the upper atmosphere, remote sensing using atmospheric radiation; solar physics, infrared astronomy, infrared signature analysis; effects of solar activity, magnetic storms and nuclear explosions on the earth's atmosphere, ionosphere and magnetosphere; effects of electromagnetic and particulate radiations on space systems; space instrumentation.

**END**

**FILMED**

3-86

**DTIC**